BMC Biology

RESEARCH ARTICLE

Open Access

Gut microbe *Lactiplantibacillus plantarum* undergoes different evolutionary trajectories between insects and mammals

Elisa Maritan[1], Marialaura Gallo[1], Dagmar Srutkova[2], Anna Jelinkova[2], Oldrich Benada[3], Olga Kofronova[3], Nuno F. Silva-Soares[1], Tomas Hudcovic[2], Isaac Gifford[4], Jeffrey E. Barrick[4], Martin Schwarzer[2*] and Maria Elena Martino[1*]

Abstract

Background: Animals form complex symbiotic associations with their gut microbes, whose evolution is determined by an intricate network of host and environmental factors. In many insects, such as *Drosophila melanogaster*, the microbiome is flexible, environmentally determined, and less diverse than in mammals. In contrast, mammals maintain complex multispecies consortia that are able to colonize and persist in the gastrointestinal tract. Understanding the evolutionary and ecological dynamics of gut microbes in different hosts is challenging. This requires disentangling the ecological factors of selection, determining the timescales over which evolution occurs, and elucidating the architecture of such evolutionary patterns.

Results: We employ experimental evolution to track the pace of the evolution of a common gut commensal, *Lactiplantibacillus plantarum*, within invertebrate (*Drosophila melanogaster*) and vertebrate (*Mus musculus*) hosts and their respective diets. We show that in *Drosophila*, the nutritional environment dictates microbial evolution, while the host benefits *L. plantarum* growth only over short ecological timescales. By contrast, in a mammalian animal model, *L. plantarum* evolution results to be divergent between the host intestine and its diet, both phenotypically (i.e., host-evolved populations show higher adaptation to the host intestinal environment) and genomically. Here, both the emergence of hypermutators and the high persistence of mutated genes within the host's environment strongly differed from the low variation observed in the host's nutritional environment alone.

Conclusions: Our results demonstrate that *L. plantarum* evolution diverges between insects and mammals. While the symbiosis between *Drosophila* and *L. plantarum* is mainly determined by the host diet, in mammals, the host and its intrinsic factors play a critical role in selection and influence both the phenotypic and genomic evolution of its gut microbes, as well as the outcome of their symbiosis.

Keywords: Gut microbiota evolution, Host–microbe symbiosis, *Lactiplantibacillus plantarum*, *Drosophila melanogaster*, Mouse, Experimental evolution, Whole genome sequencing

Background

Millions of years of co-evolution between multicellular organisms and their microbial partners have resulted in mechanisms of mutual benefits consisting of complex networks of reciprocal interactions [1–4]. One of the major melting pots of such a relationship is the

*Correspondence: schwarzer@biomed.cas.cz; mariaelena.martino@unipd.it

[1] Department of Comparative Biomedicine and Food Science, University of Padua, Padua, Italy
[2] Laboratory of Gnotobiology, Institute of Microbiology of the Czech Academy of Sciences, Novy Hradek, Czech Republic
Full list of author information is available at the end of the article

© The Author(s) 2022. **Open Access** This article is licensed under a Creative Commons Attribution 4.0 International License, which permits use, sharing, adaptation, distribution and reproduction in any medium or format, as long as you give appropriate credit to the original author(s) and the source, provide a link to the Creative Commons licence, and indicate if changes were made. The images or other third party material in this article are included in the article's Creative Commons licence, unless indicated otherwise in a credit line to the material. If material is not included in the article's Creative Commons licence and your intended use is not permitted by statutory regulation or exceeds the permitted use, you will need to obtain permission directly from the copyright holder. To view a copy of this licence, visit http://creativecommons.org/licenses/by/4.0/. The Creative Commons Public Domain Dedication waiver (http://creativecommons.org/publicdomain/zero/1.0/) applies to the data made available in this article, unless otherwise stated in a credit line to the data.

gastrointestinal tract, where trillions of microorganisms form a rich and dynamic community collectively called the "gut microbiota," which makes essential contributions to the host's health [5]. In addition to aiding digestion [2, 6] and synthesizing essential metabolites [7, 8], the gut microbiota is also involved in growth [9, 10], organ development [11], immune system maturation [12–14], inflammatory responses [15], and behavior [16]. Hence, the gut microbiota can be collectively thought of as a metabolically active organ integrated within the host [17–19].

There is immense variation in the detail of the interactions between animals and their resident microbiota. In many insects, such as *Drosophila melanogaster*, the microbiome is reported to be fairly flexible, largely environmentally determined, and less diverse than in mammals [20–29]. On the contrary, mammals harbor trillions of microorganisms in their gut, which are known to stably colonize the gastrointestinal tract already during and after birth [30–34]. Such assembly starts with low phylogenetic and species richness to culminate, over time, in the acquisition of a more complex and adult-like microbial profile [5, 35, 36]. Although gut microbes show higher resilience in mammals compared to many insects, the mammalian gut microbiota can also vary in response to both endogenous and environmental pressures [2, 37–40]. Indeed, the microbial ecosystem within the mammalian gut is shaped by the host's genetic background [41–47], together with anatomical, physiological, and immunological peculiarities [39, 48]. These include the intestinal architecture and composition [49], the host's innate and adaptive immune effectors [50–52], the host's glandular secretions (i.e., gastric acid, bile, pancreatic fluids, and enzymes), and temperature and pH [53–55]. At the same time, a plethora of environmental factors, largely related to the host's dietary habits (depending not only on nutrient components, but also on the timing and regularity of consumption), and, in case of humans, the use of drugs [56–59], the level of sanitization [37, 60], practices related to infants' delivery and feeding mode [60–62], level of exercise [63], travel [64], and geographic location [59], contribute to the variation of such a microbial ecosystem.

In this light, several studies have sought to dissect the relative contributions of these factors in shaping the gut microbiota of insects and mammals. Among these, most have stressed the importance of the host's diet as a key force in determining the microbiota configuration in both invertebrates [65–67] and vertebrates [40, 47, 64, 68–73]. In mice, switching from a low-fat, plant polysaccharide-rich diet to a high-fat/high-sugar "Western" diet can shift the microbiota structure within a single day [47], causing a progressive loss of species diversity over generations [64, 72]. Importantly, such diet-mediated microbiota alterations can ultimately result in specific microbiota–host layouts, which, in turn, affect host health and disease [69, 74].

Although these investigations have undoubtedly broadened our understanding of the diversity, resilience, and complexity of the gut microbiota across animal hosts, most of them have focused on characterizing how these external and internal factors shape microbiome compositional and functional features, eventually linking the resulting microbial pattern with a specific host trait (i.e., health or disease condition). Furthermore, by using common biomarkers (i.e., 16S rRNA), most of these studies have profiled the bacterial diversity at the genus or species level, therefore masking the potential presence of dynamic and rapidly evolving sub-populations. As a consequence, much less is known about the microbial evolutionary processes in the gut across animals. In vivo experiments, combined with deeper genome analyses, have recently brought forth a new appreciation of the gut microbes' capability of rapidly diversifying and adapting in a newly colonized environment over short [75–77] and long timescales [78], providing insights into the ecological and molecular mechanisms underlying such evolutionary paths [79–84]. In this context, *Escherichia coli* is the most widely used model bacterium for studying bacterial evolution in the mammalian gut [48, 76, 77, 80, 85]. The reasons are manifold and linked to its ecological and clinical relevance, together with ease of experimental and genetic manipulation and tractability. However, further progress into understanding the drivers of microbial evolution in the gut of different animal hosts requires us to move beyond focusing on this particular species and to look at evolution in real time across a broader range of species. This is crucial for determining the main factors governing the evolution of gut microbes.

Here, we use *Lactiplantibacillus plantarum*, a common inhabitant of the gastrointestinal tract of different animals [86], as model species to explore the evolutionary trajectories of gut microbes across animal hosts, and particularly if and how they differ between insects and mammals.

By using *Drosophila melanogaster* as an animal model, we previously demonstrated that the host's diet, rather than the host environment per se, is the predominant force in driving the emergence of the symbiosis between *L. plantarum* and the fruit fly [87]. Here, we hypothesize that, given the higher persistence and colonization ability of gut microbes in the gastrointestinal tract of mammals, the mammalian host and its intrinsic factors represent key agents of selection in the evolution of gut microbiota as compared to the mammalian host's diet. To explore this, we performed a parallel experimental evolution of

the bacterial strain *L. plantarum*^{NIZO2877}, which was previously shown to moderately promote growth both in *Drosophila* and mice [88]. We evolved *L. plantarum* in mono-association with germ-free C57Bl6 mice and in the mouse laboratory diet, separately. At the same time, we experimentally evolved the same strain in association with *Drosophila* and its nutritional environment to test if and how the presence of the invertebrate host affects the tempo and mode of evolution of its gut microbiota.

Our results indicate that the evolution of the same gut bacterium diverges between insects and mammals, pointing out the effects of the different host-derived selection pressures. While, in *Drosophila*, the host seems to benefit the fitness of *L. plantarum* in a short timescale, without significantly affecting its evolutionary trajectory, microbiome evolution in mammals follows a completely different path. Here, host factors represent a crucial agent of selection, shaping the evolution of gut microbes both on a phenotypic and genomic level. This results in an increased bacterial adaptation toward the host's intestinal environment, revealing new insights into the symbiosis between *L. plantarum* and mammalian hosts.

Results

L. plantarum evolution within a mammalian host leads to higher adaptation to the host intestinal environment

With the aim of investigating the evolutionary dynamics of *L. plantarum* in a mammalian host and to dissect the role of the mammalian host's diet in the evolution of gut microbes, we experimentally evolved the bacterial strain *L. plantarum*^{NIZO2877} (*Lp*^{NIZO2877}) in the intestine of germ-free (GF) C57Bl6 mice (Host setup) and in the mouse laboratory diet (Diet setup) separately (Fig. 1A), following the same experimental setup that we have previously applied to *Lp* evolution in *Drosophila* [87]. Specifically, in the Diet setup, we mono-associated the ancestral strain with the mouse diet in the absence of the host and monitored microbial evolution for 20 transfers (T) in five independent replicates (i.e., 20 days, corresponding to ~400 bacterial generations). In the Host setup, we mono-colonized 7 GF mice housed in cages in one Trexler-type isolator with the ancestral strain by intragastric gavage; once the mono-association had been performed, 4 female mice were bred together in one cage to generate F0 generation for the next 10 months and 2 females and 1 male were the F0 founders of the subsequent mouse generation. Bacterial evolution was followed across F0 and the subsequent generations of mice (F1, F2, F3, and F4) for 10 months (i.e., ~286 *Lp* bacterial generations; Fig. 1A, B). Evolving bacteria were horizontally dispersed and vertically transmitted across generations with no further artificial inoculation. Over this period, the mice were fed with the same diet used for the Diet setup.

Overall, *L. plantarum* growth showed a similar trend across the two evolutionary setups. In the mouse diet, we found that the microbial load increased extremely fast, as it shifted from the initial inoculum of 10^2 total CFU/mL to 3.34×10^8 CFU/mL in less than 24 h (Fig. 1B). Such a growth trend was maintained over the course of the evolution experiment, during which the bacterial load ranged between 10^7 and 10^9 CFU/mL, with the lowest value at T9 (i.e., after ~180 *Lp* generations, $\text{mean}_{T9} = 2.06 \times 10^7$ CFU/mL) and the highest at T2 (i.e., ~40 *Lp* generations, $\text{mean}_{T2} = 2.12 \times 10^9$ CFU/mL) (Fig. 1B). Microbial growth within the mouse intestine was approximately lower of 1 log CFU than that observed in the mouse diet and showed comparable loads between 50 and 200 bacterial generations, reaching the highest peak after ~110 *Lp* generations. Moreover, within each mouse generation, no significant differences were detected when comparing the initial and final bacterial concentrations (Fig. 1B). These results suggest that *L. plantarum* was able to reach and maintain high abundance both in the mouse diet and in the mouse intestine.

To compare *L. plantarum* phenotypic evolution with and without the mammalian host, we conducted a morphological analysis of the *Lp*-evolved colonies over time in both experimental setups. Interestingly, we detected the appearance of an evolved *L. plantarum* sub-population showing a different colony morphology compared to the ancestral strain in both evolutionary setups. Specifically, while *L. plantarum* typically forms rounded, smooth colonies on MRS agar, the newly evolved colonies showed a less-defined, rough morphology, which looked more transparent than the ancestral one (Additional file 1: Fig. S1). Such a population appeared after ~57 *Lp* generations in the Host setup (F0) and after ~280 *Lp* generations in the Diet setup (T14). In the mouse intestine, it initially affected 48% of the whole bacterial population, but it tended to decrease over time, reaching 38% of the population during mice Generation 3 (i.e., ~140 *Lp* generations, Additional file 1: Fig. S1). To further characterize *L. plantarum* phenotypic change, we analyzed the two bacterial morphotypes with an electron microscope. Interestingly, while the ancestral-like colonies showed a compact bacillary structure with a smooth surface, the newly evolved rough colonies had an irregular surface and looked elongated and filamentous (Additional file 1: Fig. S1B, C). However, it was unclear whether such longer chains resulted from undivided bacterial cells or whether they corresponded to single cells. Notably, when a rough colony was re-streaked on MRS agar or cultured in MRS broth, the morphology reversed to a smooth, ancestral-like one, showing that the newly evolved phenotype was transient and reversible (data not shown).

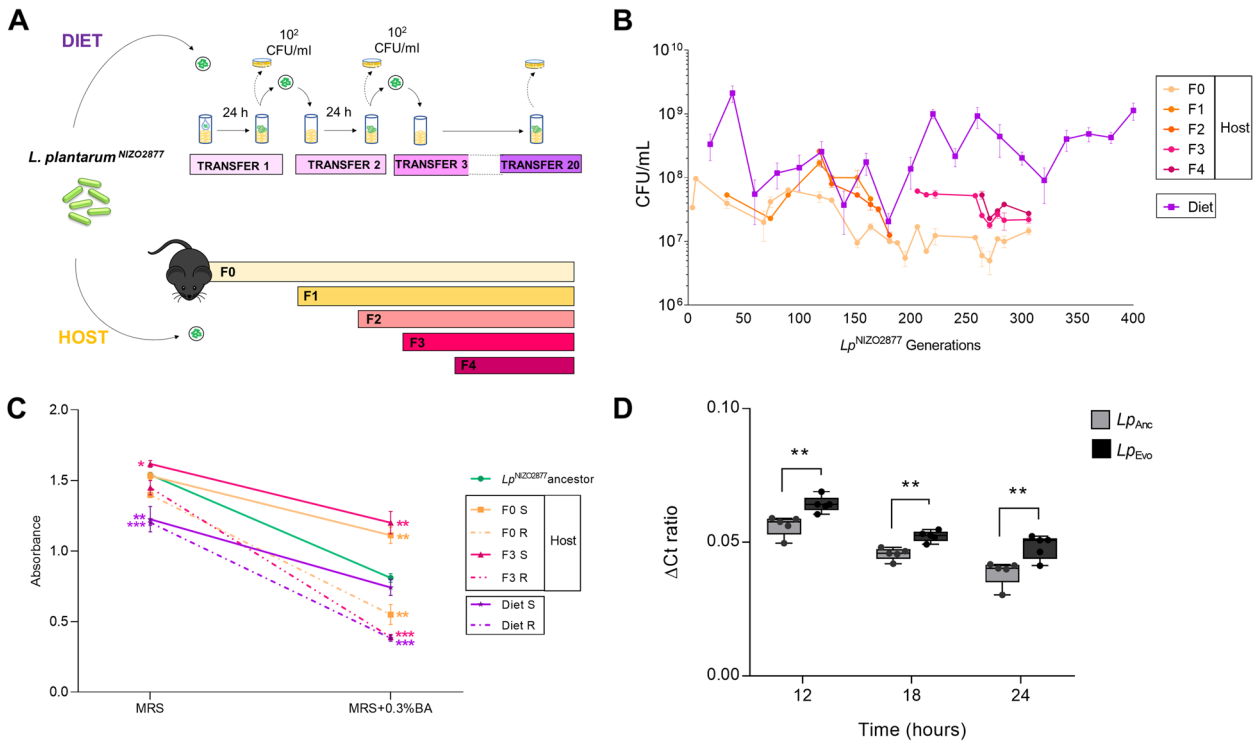

Fig. 1 *L. plantarum* evolution in mice leads to higher adaptation to the host intestinal environment. **A** Schematic representation of the $Lp^{NIZO2877}$ experimental evolution (EE) protocols in the mouse diet (Diet setup) and mouse intestine (Host setup). The ancestral strain was inoculated in the mouse laboratory diet and in the mouse intestine by intragastric gavage. Five and two replicates of EE were performed for the Diet and the Host setup, respectively. An evolved bacterial subpopulation was plated out on MRS agar plates for colony counting at different time points throughout the EE in both setups. The EE in the Diet setup was conducted up to 20 transfers (i.e., ~20 days, corresponding to approximately 400 *Lp* generations). In the mouse intestine, *Lp* EE was carried out from generation 0 (F0) to 4 (F4) of mice (i.e., 10 months after the mono-association, ~300 days, corresponding to ~286 Lp generations) for one replicate and for one generation (F0) (3 months after the mono-association) for the second replicate. Four female mice were housed in a single cage. One male and two female mice were housed in a separate single cage. **B** $Lp^{NIZO2877}$ growth trend monitored over the course of the EE in both experimental setups (Host and Diet). **C** Final absorbance values (OD = 600) reached by the *Lp* strains under standard growth conditions (MRS broth) and in MRS broth added to with 0.3% bile acids (BA). S indicates smooth colonies, while R indicates rough colonies. Each dot represents the mean of at least three experimental replicates per condition, with bars indicating the respective SD (standard deviation). For both experimental conditions (MRS broth and MRS broth + 0.3% BA), asterisks indicate significance between the final absorbance values of each strain against those of the $Lp^{NIZO2877}$ ancestor (unpaired *t* test; $*p \leq 0.05$, $**p < 0.01$, and $***p < 0.001$). **D** Quantitative PCR analysis of $Lp^{NIZO2877}$ ancestral strain (Anc) and $Lp^{NIZO2877}$-derived population (Evo) evolved in the mouse intestine. Each bar represents the standard error of the mean (SEM) of normalized ΔC_T ratios ($1/\Delta C_T$) of 3–4 mice/group. Statistical significance of the results is included (unpaired *t* test, $**p \leq 0.01$)

We next sought to investigate the mechanisms underlying the emergence of the new microbial morphotype. Bacterial morphological changes commonly occur as a result of stress responses to a wide range of factors [89–92]. In the mammalian intestine, one of the most stressful conditions is due to the activity of bile acids (BA) [89, 93–96]. We thus hypothesized that the presence of bile acids encountered during transit through the mouse gastrointestinal tract might have contributed to the appearance of the newly evolved rough morphology. On the contrary, the appearance of the rough morphology in the Diet-evolved populations could not have resulted from a stress response to bile acids, since they are absent in the mouse diet. As a consequence, we expected that both Diet-evolved colonies (rough and smooth morphotypes) would be equally affected by the presence of bile acids.

To verify these hypotheses, we first tested whether and how bile acids were able to affect *L. plantarum* growth. We serially propagated the ancestral strain $Lp^{NIZO2877}$ in MRS broth and MRS broth with the addition of 0.3% BA for 7 days and measured microbial growth. As expected, bacterial loads were significantly lower in presence of 0.3% BA compared to the control (MRS) already after one transfer ($Lp_{T1\text{-}MRS+0.3\%BA} = 4.07$

$\times 10^6$ CFUs; $Lp_{\text{T1-MRS}} = 1.75 \times 10^8$ CFUs; unpaired *t* test ***$p<0.001$) throughout the experiment ($Lp_{\text{T7-MRS+0.3\%BA}} = 8.06 \times 10^7$ CFUs; $Lp_{\text{T7-MRS}} = 3.14 \times 10^{11}$ CFUs) (Additional file 2: Fig. S2). By monitoring the bacterial morphology on agar plates, we noticed that, although the *Lp* colonies grown in the presence of BA looked slightly smaller and more transparent, the colonies maintained the ancestral smooth morphotype over the seven serial transfers (data not shown). These results demonstrate that bile acids are able to impair *L. plantarum* growth.

Next, we analyzed the fitness of Diet- and Host-evolved bacteria in the presence of bile acids and detected a *Lp*-specific response to BA depending on potential differences in the genetic background and the evolutionary history. In detail, all rough colonies reached the lowest final absorbance values in the presence of bile acids, regardless of their evolutionary history (i.e., Host- or Diet-evolved) (Fig. 1D, Additional file 3: Fig. S3 and Additional file 4: Fig. S4). They also showed a slower and delayed growth in standard MRS broth compared to the ancestor (Additional file 3: Fig. S3). Remarkably, while the Diet-evolved smooth morphotypes reached a significantly lower absorbance value compared to the ancestor (Additional file 3: Fig. S3), we detected signatures of adaptation toward bile acids among the Host-evolved smooth colonies (F0, F3). Such colonies reached, overall, the highest absorbance values in the presence of bile acids (Fig. 1C), suggesting higher tolerance to the stress compound.

To investigate whether *L. plantarum* populations evolved in the mouse intestine exhibited signs of adaptation to the animal host, mice bearing a conventional gut microbiota were gavaged either with the Lp^{NIZO2877} ancestral strain or with the Lp^{NIZO2877}-derived population evolved in the mouse intestine for 10 months (sample F0–10). Whole bacterial DNA was isolated from feces and real-time PCR was performed to track *L. plantarum* persistence over time (i.e., up to 72 h). Notably, we observed a significantly higher persistence of the *L. plantarum*-evolved population compared to the ancestral one until 24 h after gavage, while no *L. plantarum* was detected after 36 h (Fig. 1D).

Altogether, our data demonstrate that *L. plantarum* populations evolved in the mouse intestine showed adaptation towards the animal host. This, among other factors, may result from the increased tolerance to intestinal stress (i.e., presence of bile acids) and leads to higher persistence in the host intestinal environment.

Bacterial evolution within the mammalian host intestine is shaped by the emergence of hypermutators and a higher number of mutations compared to the evolution in the host diet

To investigate the influence of the mammalian animal host and its nutritional environment on the genomic evolution of its symbiotic bacteria, we sequenced the genomes of whole bacterial populations evolved in the mouse diet and in the mouse intestine at different time points. Specifically, we sequenced the genomes of fifteen *L. plantarum*-evolved populations isolated from feces pooled from 3–4 individual mice across the five generations from one replicate of experimental evolution (EE) (Additional file 8: Table S1). As for the Diet setup, we sequenced the genomes of six evolved bacterial populations isolated during transfers 2 and 14 from three independent replicates out of five (Additional file 8: Table S1). In addition, we sequenced the genomes of two single bacterial colonies: one showing the smooth, ancestral-like phenotype and the second one showing the newly evolved rough morphology (replicate 2, transfer 14, Additional file 8: Table S1).

Bacteria propagated in the mouse diet showed overall a low number of mutations, with the highest value in T14 (N= 10 mutations) (Table 1, Fig. 2A, Additional file 9: Table S2).

During this time point, the single smooth and rough colonies showed the emergence of only 1 and 3 mutations per strain, respectively (replicate 2, Additional file 10: Table S3). On the contrary, bacteria evolved in the mouse intestine revealed a marked increase in the total number of mutations compared to the Diet-evolved ones (Table 1, Fig. 2A, B, Additional file 11: Table S4). The high number of genetic variants detected in the Host-evolved *Lp* populations correlated with the appearance of novel mutations in the genes encoding for DNA replication and repair proteins *mutS* and *mutL* (methyl-directed mismatch repair complex subunits), *dnaE* (DNA polymerase III alpha subunit), and *dinB* (DNA polymerase IV) (Additional file 11: Table S4).

Mutations in the mouse host populations were overwhelmingly A:T to G:C base pair substitutions, whereas these substitutions accounted for less than 10% of mutations in the mouse diet (Fig. 2C). An elevated A:T to G:C mutational bias is consistent with mutations in *mutS* or *mutL* [97] but not *dinB* [98] or *dnaE* [99], so we concluded that defects in methyl-directed mismatch repair are probably largely responsible for the hypermutator phenotype. To test whether hypermutation of *L. plantarum* in mouse was repeatable, we sequenced the whole genome of two *Lp* populations evolved in the second replicate of experimental evolution in the mouse

Table 1 Number of mutations detected for each *L. plantarum*-evolved population

Setup	Replicate	*Lp* generation	Sample	No. of mutations
Host	1	30	F0–1	33
		60	F0–2	303
			F1–1	49
		90	F0–3	493
			F1–2	330
		110	F2–1	69
		120	F1–3	103
		150	F2–2	585
		170	F2–3	62
		200	F3–1	187
		230	F3–2	230
		240	F4–1	684
		260	F3–3	531
		280	F0–10	193
			F4–2	640
	2	30	F0–1	94
		60	F0–2	240
Diet	1	40	T2–1	2
	2		T2–2	2
	4		T2–4	2
	1	280	T14–1	6
	2		T14–2	8
	4		T14–4	10

Host setup (I replicate: F0, F1, F2, F3, and F4 generations, II replicate: F0 generation) and Diet setup (transfers 2 and 14)

intestine (F0—sequenced time points: 1, 2 months). Here, we detected 94 and 240 mutations, respectively, which included five additional variants in the *mutS* gene (Additional file 12: Table S5). This strongly suggests that hypermutation is a common evolutionary strategy of *L. plantarum* to adapt to the mouse intestine.

Whole genome sequencing of the first replicate of *Lp* EE in mice detected five separate mutations in the *mutS* gene and one in the *mutL* gene (Fig. 2D, Additional file 11: Table S4). The earliest of these mutations are a base substitution that causes an A41T amino acid substitution in *mutS* and a deletion of base pair 1303 of the *mutS* coding sequence that results in a frameshift. Secondary mutations affecting methyl-directed mismatch repair and mutations in genes involved in other DNA replication and repair processes appeared later in lineages that already had one of these two *mutS* mutations. These later mutations may have further modulated mutation rates in some cases, but we expect that these initial *mutS* mutations are responsible for most of the changes in mutation rates and spectra in the evolution experiment. In at least one case, we can predict that a secondary mutation had no effect. A point mutation in *mutS* that would lead to a D761Y amino acid substitution tracked with that of the Δ1303 mutation as soon as they both reached observable frequencies (Fig. 2D). Since this D761Y mutation is located after a new stop codon in the *mutS* gene created by the Δ1303 mutation at codon 456, it would not affect the *mutS* gene product in the context of this mutation. Therefore, we considered the A41T and Δ1303 mutations as defining two distinct *mutS* hypermutator lineages.

The two *mutS* A41T and Δ1303 hypermutator lineages and a nonmutator lineage that maintained the ancestral mutation rate competed throughout the history of the evolution experiment in different animals (Fig. 2D). The *mutS* A41T lineage appeared first and increased in frequency over the initial three months (63 generations) in the F0 mouse, reaching up to a 90% frequency. Between the third month (F0–3) and the tenth month (F0–10) however, this lineage fell below the level of detection and the *mutS* Δ1303 lineage rose to near 100% frequency. In the F3 and F4 mouse generations, the *mutS* Δ1303 lineage also ultimately swept to 100% frequency. In the F1 mouse however, neither lineage exceeded 20% frequency while, in the F2 mouse generation, both *mutS* lineages increased to ~40–50% frequency between generations 82 (F2–1) and 104 (F2–2) but then declined to less than 3% frequency by generation 123 (F2–3).

By fitting a model that assumed both *mutS* alleles evolved near the beginning of the experiment and accounted for a certain fraction of the population at each time point, we were able to estimate that the *mutS* A41T lineage accumulated mutations at a rate of 2.453± 0.146 per generation and the *mutS* Δ1303 lineage accumulated mutations at a rate of 0.310 ± 0.060 per generation (± values are standard errors of fit values). These rates are 323- and 41-fold the rate in the mouse diet treatment. The roughly 8-fold factor by which the two *mutS* lineage rates differ from one another is significant (*F*-test, $p = 2.0 \times 10^{-8}$). It may indicate that the *mutS* alleles have different effects on their own or in combination with mutations in other genes. For example, the *dnaE* mutation tracks with the *mutS* A41T allele throughout its entire history, and the *dinB* mutation appeared in this genetic background later in the F4 mouse (Fig. 2D).

By comparing the genetic variants detected in the Host- and Diet-evolved populations, we identified 5 genes that mutated in both evolutionary setups (Fig. 2A, Additional file 9: Table S2 and Additional file 11: Table S4). However, none of them persisted across generations of both conditions. We then turned our attention to those targets that exclusively mutated in the Host and Diet setups and that showed persistence across EE cycles. While within the Diet-evolved

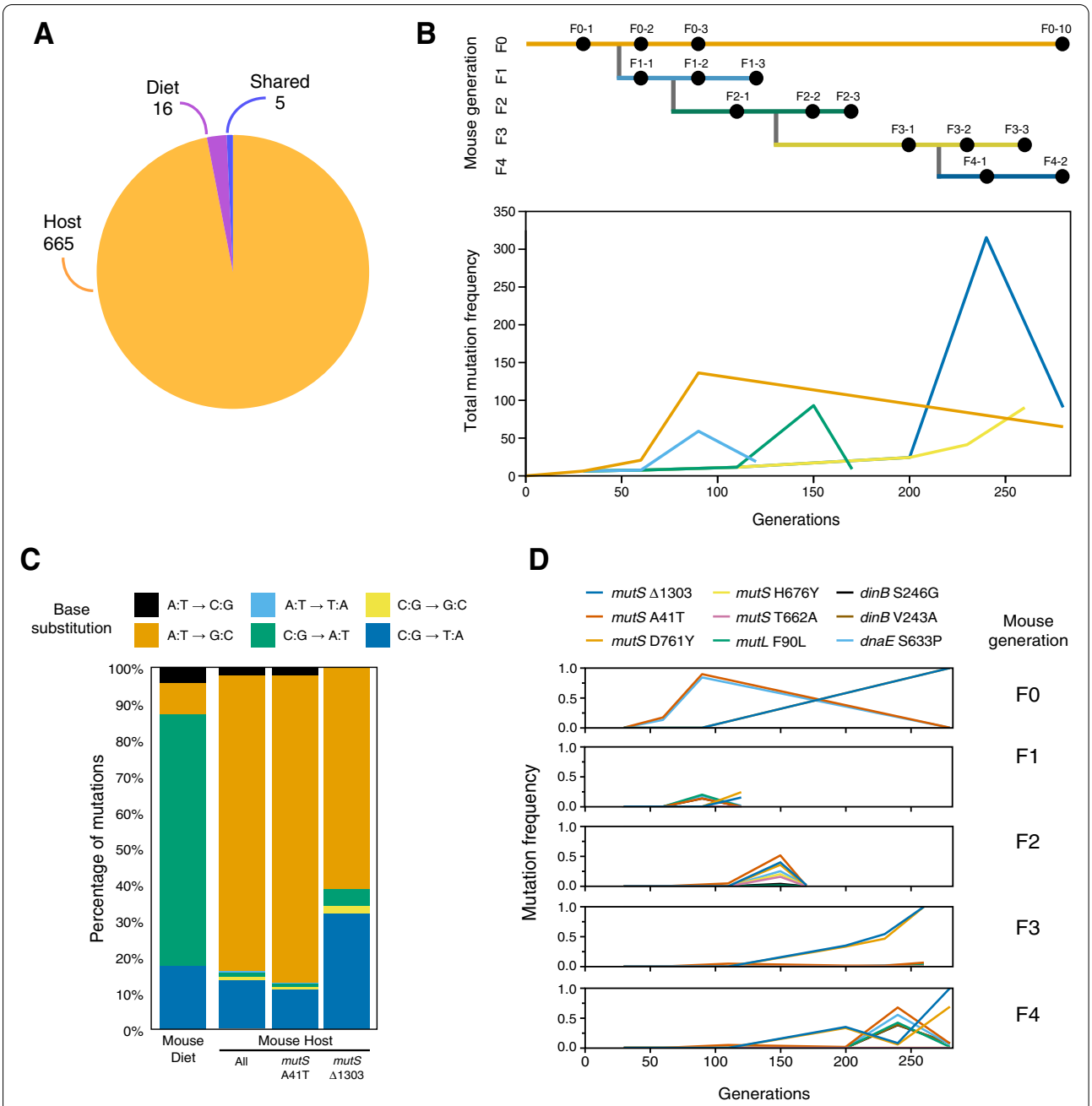

Fig. 2 Mutations that occurred during *L. plantarum* experimental evolution in mice. **A** Pie chart reporting the number of *Lp* genes that accumulated mutations over the course of each experimental evolution setup (Host- and Diet-exclusive mutations) and in both setups (shared). **B** Total summed frequencies of all mutations observed in each sample from the mouse host evolution experiment. The panel above shows the structure of the evolution experiment in mouse hosts. Bacterial populations were sequenced at the indicated time points. **C** Base substitution spectra observed in the mouse diet, as well as mouse host populations divided into all mutations and those associated with the *mutS* A41T and *mutS* Δ1303 mutator lineages (see Additional file 5: Fig. S5). **D** Frequency trajectories of the *mutS* A41T and *mutS* Δ1303 mutations and mutations in other DNA replication and repair genes (*mutL*, *dinB*, *dnaE*) that may alter mutation rates in the mouse host populations

populations, we only detected one mutation (i.e., gene: dipeptidase, Additional file 9: Table S2), the *Lp* populations evolved in the mouse intestine showed a significantly higher number of mutations ($n = 1169$; Additional file 11: Table S4), which were detected in 41 genes (and six intergenic regions). To understand whether such variants were linked to specific functions, we clustered them according to their predicted

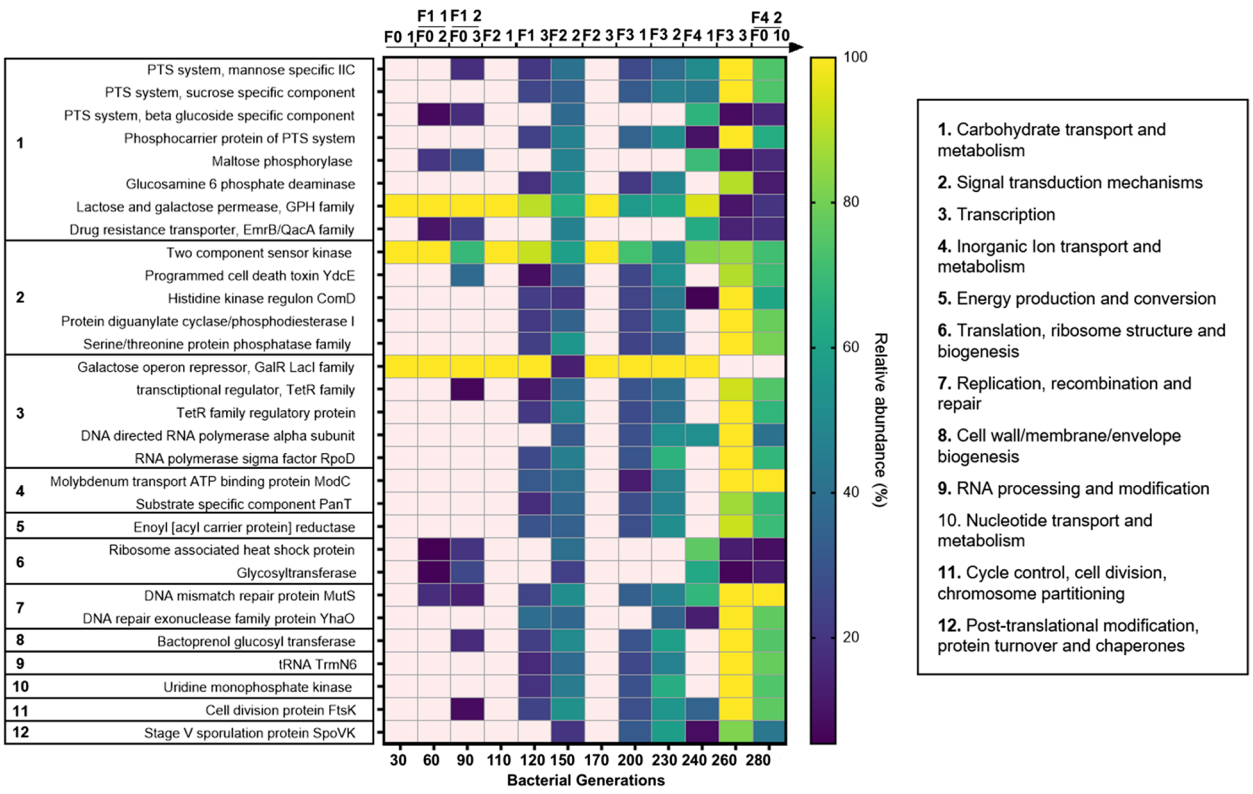

Fig. 3 *L. plantarum* genes with mutations that persisted over the course of the evolution experiment in the mouse intestine. Each target is grouped according to the predicted functional category. The colors of the heatmap indicate the relative abundance of each mutational target across time points. Lighter spaces indicate that no mutations were detected. The timeline above the heatmap represents the samples from which each *Lp* population was retrieved and sequenced

functional category. While seven of the 41 mutated genes were related to unknown functions, 30 genomic targets were grouped in 12 total functional categories, among which the carbohydrate transport and metabolism were the most enriched category (Fig. 3, Additional file 13: Table S6). Notably, four mutational targets belonging to this functional category included genes encoding for phosphotransferases system (PTS) transporters (*PTS—mannose-specific IIC, PTS—sucrose-specific IIA/IIB/IIC, phosphocarrier protein of PTS system,* and *PTS system—beta-glucoside-specific IIB/IIC/IIA component*). In addition, the genes belonging to the signal transduction and metabolism ($n = 5$) and transcription ($n = 5$) categories resulted to be affected by mutations in the Host-evolved populations (Fig. 3, Additional file 13: Table S6).

Altogether, our results demonstrate that *L. plantarum* follows divergent evolutionary paths in the mouse intestine compared to the mouse diet, both genomically and phenotypically. While *L. plantarum* evolution in the mouse diet was characterized by low mutational load, hypermutators were detected during evolution in the mouse intestine. In addition, *L. plantarum* populations evolved inside the host exhibited higher adaptation to host intrinsic factors (i.e., presence of bile salts).

Drosophila melanogaster benefits *L. plantarum* growth on a short timescale

The ecological and evolutionary dynamics of gut microbes vary greatly between mammals and insects. Among many factors, this is largely due to the different extent through which microbes colonize the gut of animals and, as a consequence, the different degrees of dependence between animals and microbes across hosts [10, 20–26, 28, 86, 100]. By using *Drosophila melanogaster* as an animal model, we have previously demonstrated that, in *Drosophila*/*L. plantarum* symbiosis, the host nutritional environment, rather than the host per se, is the predominant force in driving the emergence of such symbiosis [87]. The experimental setup was comparable to the one used in the present study to experimentally evolve *L. plantarum* in the mouse intestine and in the mouse diet. Specifically, in the Host setup, bacteria

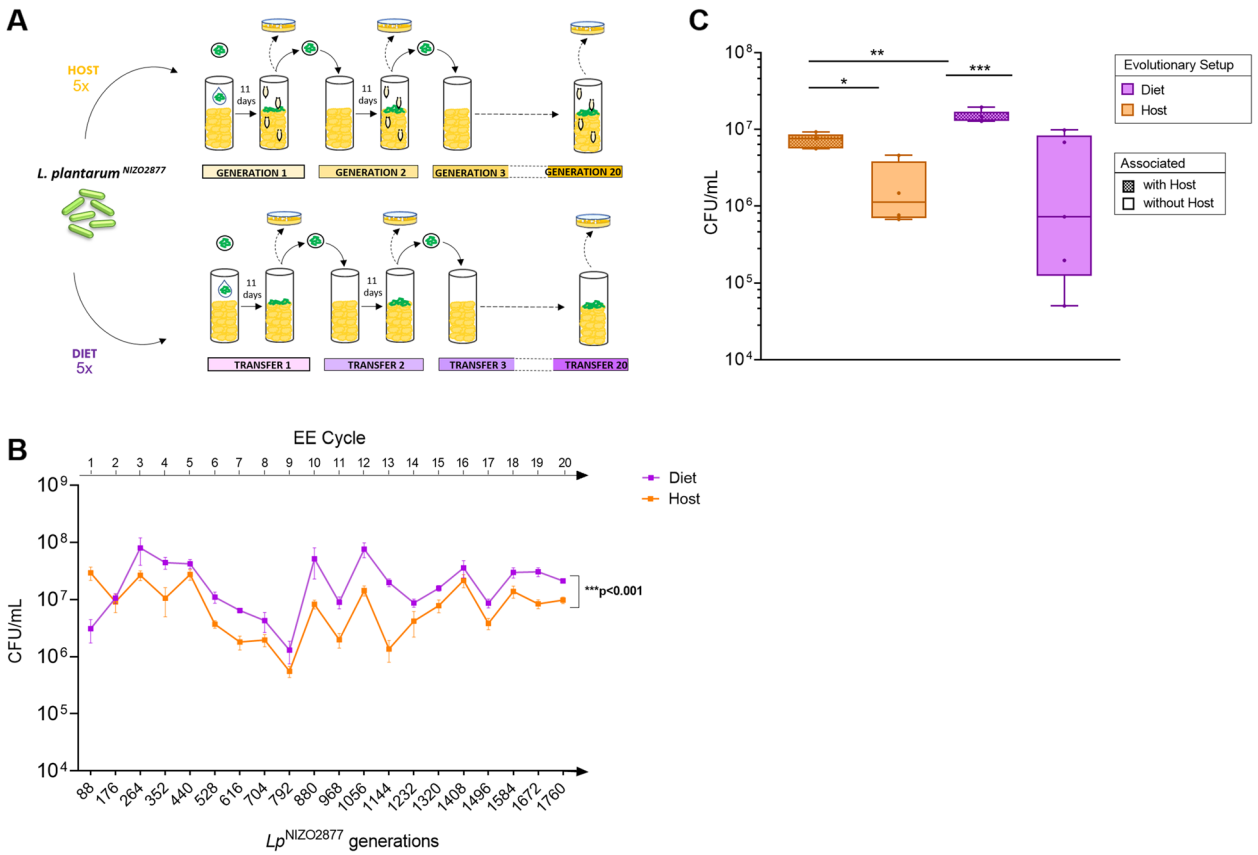

Fig. 4 *Drosophila melanogaster* benefits *L. plantarum* growth on a short timescale. **A** Design of the *Lp* experimental evolution (EE) with and without *Drosophila* (Host and Diet setups, respectively). For the first EE cycle, the ancestor strain ($Lp^{NIZO2877}$) was inoculated into tubes containing a poor-nutrient *Drosophila* diet (Diet setup) or a poor-nutrient diet containing 40 germ-free *Drosophila* embryos (Host setup). No further inoculation of the ancestor was performed until the end of the experimental evolution. As soon as at least 15 pupae emerged from all host tubes (i.e., after ~11 days, corresponding to ~88 bacterial generations), 150 µl of food was collected from both setups using a sterile loop, homogenized, and plated out to isolate bacteria (frozen "fossil" records of EE cycle 1). This bacterial population was used as the inoculum for the following generation/transfer. Subsequent EE cycles followed the same experimental procedure as cycle 1 and started from the fossil records belonging to the previous generation/transfer. The EE lasted 20 cycles (220 days, corresponding to ~1760 bacterial generations). **B***Lp* growth over the course of the Host and Diet EE protocols across 20 total EE cycles (i.e., 1760 bacterial generations). Each point represents the mean of the five experimental replicates, with bars indicating the standard error of the mean (SEM). ANCOVA ***$p < 0.0001$). **C** Microbial load obtained by mono-associating each of the five replicates of both setups (Host- and Diet-evolved bacteria) isolated from cycle 17, both with and without the host. Each bar represents the standard error of the mean (SEM) obtained by analyzing five replicate populations for each condition. Ordinary one-way ANOVA (*$p \leq 0.05$, **$p < 0.01$, and ***$p < 0.001$)

were horizontally and vertically transmitted among individuals and across generations, while in the Diet setup, artificial passages of evolving bacterial populations were conducted through experimental generations [87]. We then asked whether such differences in the selection regime between setups (natural transmission of bacteria in the Host setup versus artificial inoculation in the Diet setup) might have influenced the microbial evolutionary dynamics both in the fruit fly and in mice. To test this, we decided to replicate the *Lp* experimental evolution with and without *Drosophila* (Host and Diet setups, respectively) for a total of 20 cycles (220 days, corresponding to ~1760 bacterial generations) by applying the same transfer and sampling time for both setups (five independent replicates per setup, Fig. 4A). In this way, we were able to minimize differences between setups so that the microbial evolutionary trajectories relied exclusively on the presence/absence of the animal host.

We first investigated whether the presence of *Drosophila* affected $Lp^{NIZO2877}$ evolution by conducting morphological evaluations of the evolved bacterial populations and analyzing the microbial growth dynamics throughout the two experimental protocols. Specifically, the evolved bacterial populations in the ten

independent replicates have been plated out at the end of each experimental cycle (total of 20 cycles), macromorphological evaluation of bacterial colonies was routinely performed and microbial load was measured at the end of each cycle (~11 days). Contrary to what we observed during *L. plantarum* evolution in the mouse intestine, no differences in colony morphology were observed across the *Lp* populations evolved with and without *Drosophila*. Remarkably, the microbial load was significantly higher overall in the absence of the host, except for in the first generation (i.e., 88 bacterial generations) (Fig. 4B). Since the difference in microbial growth between the two setups was detected at a specific time point (i.e., the end of each experimental generation—11 days), we asked whether the higher microbial load observed in the Diet setup resulted from a delayed growth dynamic compared to that of the Host-evolved populations. To address this question, we analyzed the microbial concentration at an earlier time point (i.e., 7 days after the mono-association). The *Lp* concentration was confirmed to be overall significantly higher in the absence of the host, except for generations 6, 19, and 20 (i.e., after ~528, 1672, and 1760 bacterial generations, respectively) (Additional file 6: Fig. S6).

Interestingly, throughout our sampling period, we also noticed an unexpected correlation between the growth dynamics of the Host- and Diet-evolved populations, which was particularly pronounced from generations 6 to 12 (i.e., from 528 to 1056 $Lp^{NIZO2877}$ generations) (Fig. 4B). To test the repeatability of our findings, we replayed *L. plantarum* EE from cycles 5 to 12 in both setups and analyzed the microbial concentration after 7 and 11 days. Our results further confirmed the correlation in microbial growth dynamics between the Host and Diet setups (Additional file 6: Fig. S6). This demonstrates that *Lp* growth dynamics are repeatable and did not result from experimental artifacts or external variables.

We then asked whether and how *Lp* evolutionary history (i.e., evolving in the presence or absence of its host) could generate evolutionary tradeoffs in a different environment. To this end, we mono-associated *Lp* Host- and Diet-evolved populations isolated at the end of EE cycle 17 from each of the ten independent replicates (five replicates per setup), both in the presence and absence of *Drosophila* and analyzed the microbial load in both conditions after 11 days. *Lp* concentration was always significantly higher in the presence of *Drosophila* (Fig. 4C). This was also visible after cycle 1 of *Lp* EE (i.e., ~88 *Lp* generations; Fig. 4B). However, when comparing the microbial evolutionary backgrounds, the Diet-evolved populations reached significantly higher loads compared to the Host-evolved populations when associated with the fruit fly (Fig. 4C). Taken together, our results show that, although *Drosophila* benefits *L. plantarum* growth on a short timescale, bacterial evolution ultimately leads *L. plantarum* to grow to a higher extent in the absence of *Drosophila*.

Genome sequencing reveals parallel genomic evolution between *Lp* populations evolved with and without *Drosophila*

We next investigated if and how *Drosophila* influences *Lp* evolution on a genomic level. To do this, we performed metagenomic sequencing of bacterial populations isolated from both experimental setups during EE cycles 2, 8, 14, and 20 (three independent replicates sequenced per time point and setup, Additional file 8: Table S1). Across the two evolutionary setups, we detected a similar mutational trend in terms of the number of genetic variants (Table 2, Fig. 5A, B) and identified signatures of strong parallel genomic evolution. Bacteria evolved in the fly host populations accumulated 0.00177 ± 0.00018 mutations per generation and fly diet populations accumulated 0.00150 ± 0.00010 mutations per generation (± values are standard errors of fit values). These rates did not differ significantly from one another (*F*-test, $p = 0.059$). Mutations in the fly host and diet populations were mainly C:G to A:T and C:G to T:A substitutions (Fig. 5C).

Three genes mutated in both setups (i.e., *ackA*, *rho*, and *gltL*, Fig. 5D, Additional file 14: Table S7 and Additional file 15: Table S8). Specifically, all *Lp* experimental replicates isolated from the Host and Diet setups showed at least one genomic change within the acetate kinase A gene (*ackA*), which was the first gene to be affected by

Table 2 Number of mutations detected for each *L. plantarum*-evolved population in the fly Host and Diet setups

EE cycle	Sample	No. of mutations Host setup	No. of mutations Diet setup
2	1	3	8
	2	8	10
	4	7	5
8	1	10	7
	2	8	10
	4	6	6
14	1	11	10
	2	11	14
	4	10	8
20	1	8	7
	2	6	12
	4	10	4

EE experimental evolution, *Sample* replicate

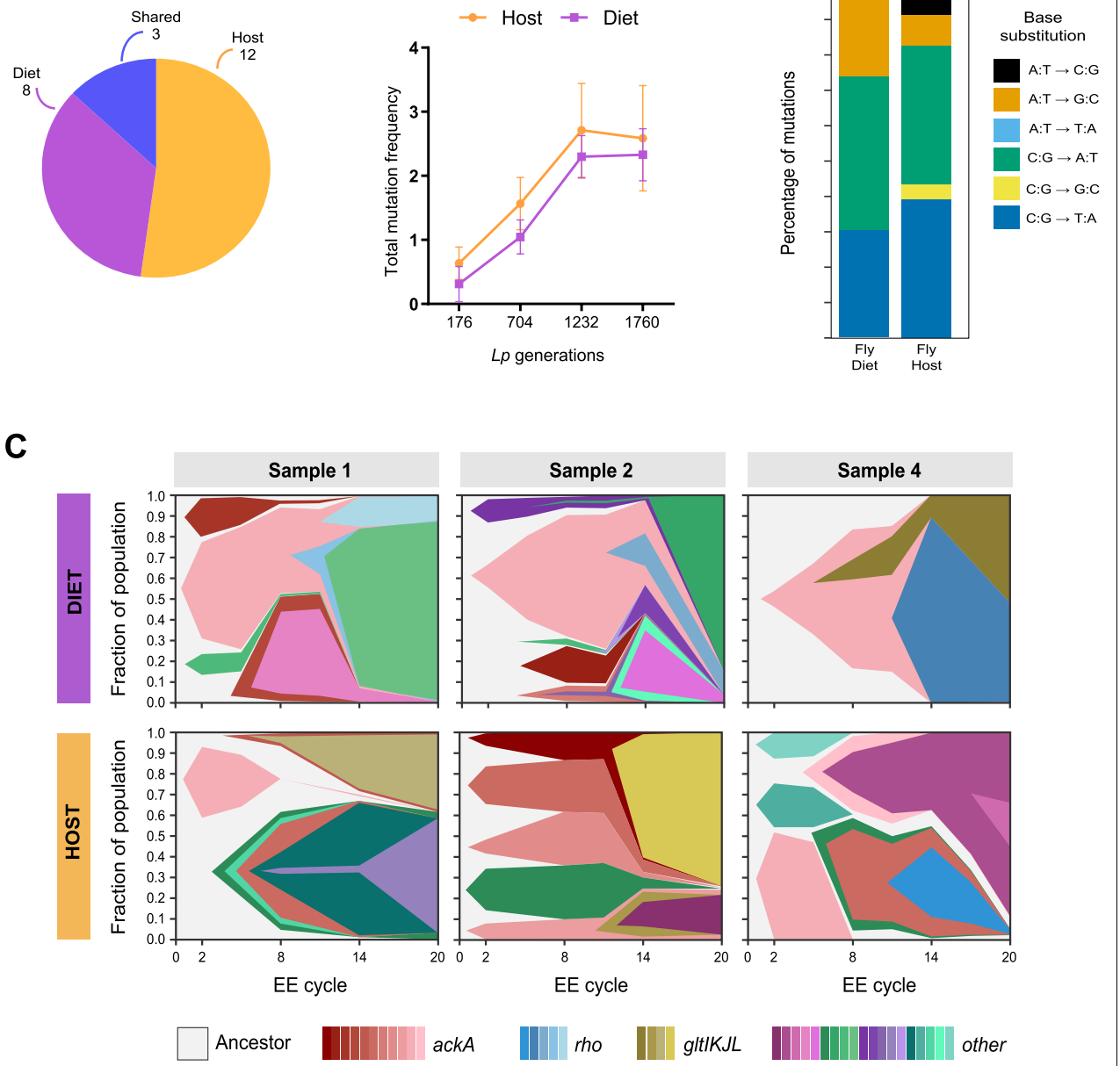

Fig. 5 Mutations occurred during *L. plantarum* experimental evolution in the fly setup. **A** Pie chart reporting the number of *Lp* genes that accumulated mutations over the course of each experimental evolution setup (Host- and Diet-exclusive mutations) and in both setups (Shared). **B** Total summed frequencies of all mutations observed in each sample from the Host and Diet evolution experiment. Each point represents the mean of the 3 experimental replicates analyzed, with bars indicating the standard deviation (SD). **C** Base substitution spectra observed in the fly host and diet. The total number of mutations detected in each group (*N*) is shown above each bar. **D** Dynamics of mutations in fly diet and host treatments. Muller plots representing the evolutionary dynamics of *Lp* genes that mutated in the Host and Diet-evolved populations across EE cycles 2, 8, 14, and 20 (i.e., after 176, 704, 1232, and 1760 *Lp* generations)

mutation and exhibited the highest number of mutations per gene (Fig. 5D, Additional file 14: Table S7 and Additional file 15: Table S8). This result confirms our previous work showing that mutations of *L. plantarum ackA* occur both in the presence and in the absence of *Drosophila*. We identified 12 non-synonymous *ackA* mutations, one of which was shared between the Host and Diet setups. The shared variant appeared during EE cycle 2 (i.e., after

176 bacterial generations), reaching fixation in all Diet-evolved populations (Fig. 5D, Additional file 14: Table S7 and Additional file 15: Table S8), while it disappeared in the Host-evolved populations. Here, it was replaced by multiple additional variants within the same gene. At the same time, we detected mutations that exclusively occurred in each evolutionary setup. Specifically, 13 genes mutated in the Host-evolved populations at least once, while 9 exclusive mutational targets were detected in the Diet-evolved populations (Fig. 5A, D, Additional file 14: Table S7 and Additional file 15: Table S8). Altogether, our results show that *L. plantarum* undergoes parallel genomic evolution with and without its invertebrate animal host, further demonstrating that, contrarily to what we observed in *L. plantarum*/mouse symbiosis, in the relationship between *L. plantarum* and the fruit-fly, the host nutritional environment largely dictates the microbial evolutionary trajectories both genomically and phenotypically.

Discussion

Given the complexity of host–microbial symbioses and the high variability that characterizes such associations in natural environments, understanding the evolutionary trajectories of gut microbes across different symbiotic relationships is of particular interest. In this work, we coupled experimental microbial evolution with genome sequencing and phenotypic characterization to explore the evolutionary path of *Lactiplantibacillus plantarum*, a common animal gut commensal, in vertebrate (mouse) and invertebrate (*Drosophila melanogaster*) animal models. We previously demonstrated that, in the symbiosis between *Drosophila* and *L. plantarum*, the nutritional environment is the main selective agent in the evolution and adaptation of the commensal bacterium [87]. Here, we asked if and how *L. plantarum* evolution varied in the context of its symbiosis with mammalian hosts, where gut commensals exhibit higher levels of colonization and mutualistic interactions are reported as more persistent than those observed in insects [23, 32]. Although diet is well known to largely dictate gut microbes' evolution in mammals [47, 84], disentangling the respective roles of nutritional and host factors in such processes is challenging. To address this, we tracked *L. plantarum* phenotypic and genomic evolution in the mouse intestine and in their diet.

L. plantarum growth dynamics in the presence and absence of the mammalian animal host were similar between the two evolutionary setups (Fig. 1B). We believe that, in the Diet setup, the fast and high microbial persistence can be explained by considering the structure of our experimental setting (i.e., bacterial re-inoculation at the beginning of each EE cycle), a result that was not expected in the presence of the host. Here, bacterial administration was performed at the beginning of the experimental evolution and bacteria were transferred vertically and horizontally among mice, without any further external input. In addition, the complex physical and chemical conditions encountered during transit through the mammalian gastrointestinal tract usually provide a challenge to the commensal microbiota attempting to colonize the host GI niche [101, 102]. Here, the innate immune system of the host, the food transit, and the plethora of antimicrobial compounds secreted into the gut (including hydrochloric acid, bile, hydrolytic enzymes, and antibodies), as well as other ecological factors, such as the intense microbial competition for space and nutrient resources, represent obstacles to both bacterial colonization and survival [103, 104]. We speculate that the high bacterial concentration observed in the Host setup is directly linked to the use of mono-colonized mice. It will be interesting to assess the *Lp* evolutionary growth dynamics in mice harboring a complex microbial community. *L. plantarum* adaptation to the mammalian host was also visible by the increased tolerance under bile acid stress and the higher persistence in the mouse intestine exhibited by the *Lp* populations evolved in the Host setup (Fig. 1C, D, Additional file 3: Fig. S3 and Additional file 4: Fig. S4). This suggests that, while facing the adverse conditions along the mouse GI tract, some bacterial subpopulations gradually adapted to the host intrinsic factors, resulting in improved growth, fitness, and colonization ability.

During *Lp* experimental evolution in the mouse setup, we also detected a morphological transition of bacterial colonies, characterized by the emergence of a rough phenotype that occurred both in the Host and Diet setups. Morphological transitions within a single strain population, known as pleomorphism [105], often occur in bacteria evolution and have been reported by several studies as an adaptive strategy for survival in response to fluctuating environments, especially to limiting or changing growth conditions. Moreover, *L. plantarum* had already been shown to exhibit a rough surface and cell elongation under a wide range of stress environments, including heat and ethanol shocks [106–108], presence of nitrite [109], low pH [91, 107], lactic acid stress [110], nutrient stress [111], and bile stress [89]. Interestingly, when observed with an electron microscope, the rough colonies exhibited a filamentous and chaining phenotype (Additional file 1: Fig. S1B, C). In this regard, it is worth noticing that the Diet-evolved strains exhibiting the rough morphology showed a mutation in a gene encoding for the cell division protein DivIVA (Additional file 10: Table S3). DivIVA is a coiled-coil protein first discovered in *Bacillus subtilis* and highly conserved among Gram-positive

bacteria. It clusters at curved membrane areas such as the cell poles and invaginations that occur during cell division, where it serves as a scaffold protein for the recruitment of Min proteins, which spatially regulate the division process [112, 113]. In contrast to *B. subtilis*, where the deletion of the *divIVA* gene was responsible for the formation of a filamentous and mini-cell phenotype [114], ΔdivIVA mutants of *Listeria monocytogenes* exhibited a pronounced chaining phenotype [115]. Although these cells had clearly completed cell division, they remained attached even after completion of cross-wall synthesis. This indicates that the deletion of *divIVA*, although not affecting cell division per se, might affect the post-divisional separation of daughter cells. However, further evidence of *divIVA* functioning within *L. plantarum* species is needed to assess our hypothesis, considering that the functionality of *divIVA* has been shown to be species-specific [113]. We next investigated the cause of the emergence of the rough morphotype. Even if we cannot assess whether the pleomorphism that emerged from both the Diet- and Host-evolved rough colonies was due to the same stress factor, it is interesting to note that all rough colonies had reduced vitality and increased susceptibility to bile acids stress compared to the smooth ones, regardless of their evolutionary history (i.e., Host- or Diet-evolved) (Fig. 1C, Additional file 3: Fig. S3 and Additional file 4: Fig. S4). This is consistent with other findings, showing that the gradually increasing severity of changes in *L. plantarum* morphology coincide with a respective decrease in the bacterial growth rate [89].

Genome sequencing of *Lp* evolved with and without its mammalian host revealed weak parallelism. The Diet-evolved populations showed a significantly lower number of mutations, among which only one persisted over time (*Dipeptidase* gene). On the contrary, we detected several mammalian host-specific mutational targets, most of which are involved in carbohydrate transport and metabolism (Fig. 3, Additional file 4: Fig. S4). Among these, four genes belong to the phosphotransferases system (PTS), a highly conserved bacterial phosphotransferase cascade whose components modulate many cellular functions in response to carbohydrate availability [116] and which has already been observed to be over-expressed or mutated in other mouse gut colonization experiments [76, 86, 117]. This is in line with a recent study showing that *L. plantarum* convergently evolves across vertebrate animal hosts (i.e., human, mouse, zebrafish) by acquiring mutations primarily modulating carbohydrate utilization and acid tolerance [118].

Notably, *Lp* genomic evolution within the mouse intestine was repeatedly characterized by the emergence of hypermutators carrying multiple mutations in the *mutS*, *dnaE*, and *dinB* genes (Fig. 2B, D), which were not observed in any of the Diet-evolved populations. These genes are involved in the DNA mismatch repair system and DNA replication accuracy [119–121]. Mutations in these regions can lead to up to a 100-fold increase in the spontaneous mutational rate compared to their wild-type counterparts [122–125] and have already been observed in clinical, environmental, and laboratory microbial populations, suggesting that the evolutionary strategies of bacteria include systems for increasing mutability [126, 127]. In the context of the mammalian gut, most of the experimental research has been carried out using *E. coli*. With this species, spontaneously arising mutator bacteria can also quickly become dominant during the course of gut colonization [76, 80, 83, 85, 128]. Such an advantage depends on the ability of the hypermutators to generate adaptive mutations rather than on the beneficial pleiotropic effects of the mutator allele, suggesting that adaptive mutations are fixed rapidly in mutator populations. Indeed, while in stable environments the maintenance of a low mutational rate is fundamental to avoid deleterious mutations that might lead to species loss, several experimental studies, performed both in vitro [129, 130] and in vivo [85, 131], have shown that increased mutational rates can be beneficial to bacterial populations facing unpredictable adverse conditions, where mutations might help cells to overcome selective pressures [126, 132]. At the same time, it has been shown that a high mutation rate can be initially beneficial because it allows faster adaptation, but this benefit disappears once adaptation is achieved [80, 85]. Although we did not assess whether the high mutation rate observed within the Host-evolved *Lp* populations is directly responsible for adaptive mutations in the mouse intestine, our results showed that the hypermutator lineages persist longer in the mouse intestine compared to the ancestral population (Fig. 1D). Nevertheless, the elevated mutation rate, as well as other events commonly observed in studies of gut microbe evolution (e.g., clonal interference, epistasis, horizontal gene transfer) might mask signatures of adaptation, making it difficult to separate selection from drift [77, 80, 85, 133, 134]. From this standpoint, understanding the role of persisting mutations and their effect on gut microbiota fitness and physiology might be of great interest to further dissect their consequences on the evolution of the symbiosis between bacteria and its mammalian animal host.

The divergent trajectories detected by comparing *L. plantarum* evolution in a mammalian host and in its diet are in contrast with *L. plantarum* evolutionary dynamics observed in *Drosophila*, where we have previously demonstrated that gut microbes undergo parallel evolution in the presence and absence of the fruit fly [87]. This indicates that selection regimes were comparable

in the two environments. Specifically, in the Host setups, bacteria were horizontally and vertically transmitted among hosts (both in mice and *Drosophila*), while in the Diet setups, artificial passages of the evolving bacterial population were performed. However, we acknowledge that the experimental differences in bacterial propagation between the Host and Diet setups might not allow a direct comparison of the bacterial evolutionary dynamics.

To address this issue, in this work, we replayed *L. plantarum* experimental evolution in *Drosophila* by applying the same transferring and sampling time in both setups. This allowed us not only to demonstrate that the parallelism between *Lp* populations evolved in the presence of *Drosophila* and in its nutritional environment is repeatable, regardless of the experimental selection regimes used, but also to provide new insights into the respective role of the invertebrate host in the evolutionary path of *L. plantarum*. Indeed, we detected host-specific mutations that occurred in a later stage of bacterial evolution and showed persistence across EE cycles (Additional file 15: Table S8.). These genes mainly belong to bacterial immune evasion pathways, amino acid transport, and metabolism. Specifically, *Lp* Host-evolved populations were repeatedly affected by non-synonymous mutations of the *mprF* gene, which encodes for an *L-O-lysylphosphatidylglycerol synthase*, an enzyme that is present in both Gram-positive and Gram-negative bacteria [135] and catalyzes the transfer of a lysyl group to the negatively charged phosphatidylglycerol (PG), a major component of the cytoplasmatic membrane [136, 137]. This reaction modifies the net charge of PG, neutralizing the membrane surface and thus significantly impacting the interactions with cationic antimicrobial peptides (CAMPs) produced by the host's immune system (defensins and cathelicidins). Accordingly, the loss of Lys-PG in *mprF* mutants has been shown to lead to an increase in bacterial susceptibility to a broad variety of cationic antimicrobial peptides [138] in different bacterial species [139–141], thereby demonstrating a general role of mprF in bacterial immune evasion. In addition, non-synonymous Host-specific mutational targets also include *glnQ*, encoding a glutamate transport ATP-binding protein, which is involved in glutamate uptake in other Gram-positive bacteria [142], and *glnA* (encoding for a glutamine amidotransferase), involved in amino acid transport and metabolism. Specifically, glutamine amidotransferases (GATase) are enzymes that catalyze the removal of the ammonia group from a glutamine molecule and its subsequent transfer to a specific substrate, thus creating a new carbon–nitrogen group on the substrate. It is important to notice that, although such mutations were detected only in Host-evolved *Lp* populations, they ultimately did not confer a fitness advantage in the presence of the host, as Diet-evolved populations ultimately reached higher loads when associated with the fruit fly (Fig. 4B). These results differ from other previous findings, according to which *Drosophila* has a positive impact on the growth of its gut microbiota [26]. To further investigate this point, we compared the growth of the two *Lp*-evolved populations in both experimental setups (Host and Diet). Notably, we found that the *Lp* concentration was always significantly higher in the presence of *Drosophila*. However, the Diet-evolved bacteria had an overall growth advantage compared to the Host-evolved populations when associated with the fruit fly (Fig. 4C). Interestingly, this result was already visible from the *Lp* growth dynamics monitored during the experimental evolution (Fig. 4B), where *Lp* was retrieved in a higher concentration in the presence of the fly only in the early stages (~88 *Lp* generations, EE cycle 1).

Taken together, our results suggest that the fly improves *Lp* growth in a short ecological timescale, that is in the absence of evolution, regardless of the microbial evolutionary background. On the other hand, bacterial growth is favored in the absence of its fly host in the longer term. We speculate that such different growth dynamics might be due to a combination of factors. On the one hand, the growth advantage initially conferred by the fly host to its microbiota might result in an evolutionary "relaxed" selective environment, which in turn affects bacterial growth and adaptation. On the other hand, the stronger selection occurring in the absence of the fly host might ultimately result in higher bacterial fitness in a longer timescale. Indeed, it is commonly expected that the rate of adaptation is higher when selection is stronger [143]. At the same time, it is worth noticing that the lower microbial load detected in the presence of the host might be partly due to the continuous ingestion of bacteria by the fruit fly, as it is known that a large fraction of ingested bacteria gets killed while passing through the stomach-like region of the *Drosophila* gut [26, 144, 145]. However, this does not fully explain the higher *Lp* loads retrieved in the absence of the host, as it should have been visible already during the first EE cycle (Fig. 4B).

Conclusions

Our results demonstrate that *L. plantarum* evolution diverges between insects and mammals. Specifically, we show that in *Drosophila*, the nutritional environment dictates microbial evolution, while the host benefits *L. plantarum* growth only over short ecological timescales. By contrast, in a mammalian animal model, *L. plantarum* evolution results to be divergent between the host intestine and its diet, both phenotypically (i.e., Host-evolved populations show higher adaptation to the host intestinal

environment) and genomically. Here, both the emergence of hypermutators and the high persistence of mutated genes within the host's environment strongly differed from the low variation observed in the host's nutritional environment alone. This indicates that the mammalian animal host, together with host's intrinsic factors, represent crucial agents of selection for the evolutionary path of gut microbes. In addition, we believe that ecological factors need to be considered in the interpretation of our findings. Specifically, gut bacteria in flies are largely environmentally determined, as flies live in their nutritional environment. On the contrary, mammalian gut microbes are known to stably colonize the host intestine and their dispersal strongly relies on cohabitation and host-mediated transmission. Altogether, such ecological drivers contribute to the divergent evolutionary trajectory of gut microbes across animals, beyond the selective pressure exerted by the host per se. Furthermore, we believe that increasing the number of independent replicates of bacterial experimental evolution in the mouse intestine would be needed to further demonstrate the replicability of our findings. From this standpoint, the key questions we need to address in future studies should center on the characterization of the targets of selection, as well as the factors driving the gut microbes' adaptation from a subspecies level to higher levels of microbial interactions. Addressing this will allow us to better understand the relationship among evolution, adaptation, and microbial function and will reveal the principles that govern the colonization success, persistence, and resilience of gut microbes and how they vary across animals and humans.

Methods

Bacterial strains and culture conditions

All strains used in the present study were derived from the ancestor *L. plantarum*^{NIZO2877} that was originally isolated from a sausage in Vietnam [146]. At the end of each experimental evolution transfer or generation, the evolved strains were stored at −80°C in 1 mL of phosphate-buffered saline (PBS, Sigma) by adding 200 µL of 80% glycerol.

Drosophila stocks and breeding

Drosophila yw flies were used as the reference strain in this work. *Drosophila* stocks were cultured at 25°C with 12/12-h dark/light cycles on a yeast/cornmeal medium containing 50g/L inactivated yeast (rich diet) as described by Storelli et al. [10]. Poor-nutrient diet was obtained by reducing the amount of yeast extract to 8 g/L. Germ-free (GF) stocks were established and maintained as described in Storelli et al. [10].

Drosophila diet

The fly diet used in the present study was a poor yeast diet containing 8 g inactivated dried yeast, 80 g cornmeal, 7.2 g agar, 5.2 g methyl 4-hydroxybenzoate sodium salt, and 4 mL 99% propionic acid per 1 L. After preparation, fly food was poured in 50-mL tubes by adding 10 mL of food to each tube.

Mouse diet

For mouse breeding and for in vitro *Lp* evolution we use mouse breeding extrudate diet V1126-000 (Ssniff, Soest, Germany). The diet was vacuum packed and sterilized by gamma-irradiation (25 kGy, Bioster, Czech Republic). It is a grain-based diet consisting of wheat, soybean products, corn (maize) products, oat middlings, minerals, soybean oil, sugar beet pu*Lp*, vitamins and trace elements, L-lysine HCl, and DL-methionine. For the experimental transfer of *Lp*^{NIZO2877} in the mouse diet, the food was manually crushed, as it was initially provided in the form of pellets.

L. plantarum experimental evolution in mice

Germ-free (GF) C57Bl6 mice were kept under axenic conditions in Trexler-type plastic isolators, and the absence of aerobic and anaerobic bacteria, molds, and yeast was confirmed every 2 weeks by standard microbiological methodology [88]. The mice were kept in a room with a 12-h light–dark cycle at 22°C, fed an irradiated sterile diet V1126-000 (Ssniff, Soest, Germany), and provided sterile autoclaved water ad libitum. *L. plantarum*^{NIZO2877} was grown in De Man, Rogosa and Sharpe (Oxoid) in static culture overnight at 37°C for the monocolonization of GF mice. Set up of the first replicate of EE: Seven 12-week-old GF mice (1 male and 6 females) were colonized with a single dose (2×10^8 CFU/200 µL PBS) by intragastric gavage to create F0 generation. Four female mice were housed in a single cage. One male and two female mice were housed in a separate single cage. Evolving bacteria were horizontally dispersed and vertically transmitted with no further artificial inoculation. The stability and level of colonization was checked periodically by plating of appropriate feces dilution collected from 3–4 mice on MRS agar and counting after aerobic cultivation for 48 h at 37°C (CFU/mL). After verification of stable colonization, mice were mated and colonization of F0 and subsequent generations (F1, F2, F3, F4) was followed for 10 months. Fecal pellets were collected and pooled from 3–4 mice for the duration of the entire experimental evolution (10 months), diluted in PBS 1X, and plated in MRS agar to isolate the evolving *L. plantarum* colonies in order to follow their evolution along time or stored with 20% glycerol at −80°C for

future analysis. Set up of the second replicate of EE: Two 12-week-old GF female mice were colonized with a single dose (2×10^8 CFU/200 µL PBS) by intragastric gavage. Each mouse was housed in a single cage inside an isolator. There was no further artificial inoculation. The stability and level of colonization was checked periodically by plating of appropriate feces dilution collected from each mouse on MRS agar and counting after aerobic cultivation for 48 h at 37°C (CFU/mL). Fecal pellets were collected and stored with 20% glycerol at −80°C for future analysis. The animal experiments were approved by the Committee for the Protection and Use of Experimental Animals of the Institute of Microbiology of the Czech Academy of Sciences.

L. plantarum experimental evolution in the mouse diet

The experimental evolution of *L. plantarum*^{NIZO2877} in the mouse laboratory diet was designed as follows: *Lp*^{NIZO2877} (ancestor) was cultivated at 37°C overnight in 10 mL of MRS Broth. On the following day (day 0), 1 mL of the overnight culture was centrifugated at 4000 rpm for 10 min and washed in sterile PBS. After proper dilutions, 10 µL of PBS-washed culture of *L. plantarum* (corresponding to 10^2 total CFUs) was inoculated in microtubes (five total technical replicates) containing 150 mg of the crushed mouse laboratory food supplemented with 100 µL of sterile deionized water. At the same time, 100 µL of the bacterial inoculum was plated out on MRS Agar and grown at 37°C for 48 h as a control. To mimic the host's intestine condition, bacteria were incubated at 37°C for 24 h. On the following day (day 1), the evolved bacteria of transfer 1 (T1) were isolated from each of the five replicates of the mouse diet. Specifically, the medium was crushed using the Tissue Lyser II (Qiagen) (frequency of 30 Hz for 40") in 1 mL of PBS microtubes containing 0.75/1-mm glass beads. A total of 10 µL of the crushed medium (10^2 total CFUs) was used to inoculate five novel sterile medium microtubes (day 0 of T2). This allowed the propagation of an evolving bacterial subpopulation derived from the ancestor on the new medium. To determine the microbial load reached at the end of the first transfer (day 1 of T1), 100 µL of the crushed medium was plated out on MRS agar at 37°C for 48 h. Each experimental transfer followed the same experimental setup as the one described above, with the exception that, since bacteria were propagated along with the food, no further inoculation of the ancestor strain *Lp*^{NIZO2877} was performed. The EE in the mouse diet was conducted for a total of 20 transfers.

L. plantarum experimental evolution in *Drosophila*

Two EE protocols were performed simultaneously to evolve *L. plantarum*^{NIZO2877} in the presence of both *Drosophila* and its diet (Host setup) or just with its diet (Diet setup). For the first generation of both setups, *L. plantarum*^{NIZO2877} was cultured overnight in 10 mL of MRS broth at 37°C. At the same time, GF female flies had been placed inside cages containing poor-nutrient GF medium to lay eggs. On the following day, 40 embryos were transferred to 5 replicate tubes containing poor-nutrient diet (Host setup). Five tubes containing poor-nutrient diet were also used for the Diet setup, with the exception that no *Drosophila* eggs were added in this case. *Lp*^{NIZO2877} overnight culture was washed in sterile PBS and after proper dilutions 1 mL of PBS-washed culture was added directly on the eggs and the fly food (bacterial inoculum = 10^5 CFU/mL). No further inoculation of the ancestor strain *Lp*^{NIZO2877} was performed after the beginning of the first generation until the end of the experimental evolution. Once the mono-association had been performed, Host and Diet tubes were incubated at 25°C. As soon as at least 15 pupae emerged from all Host tubes, 150 mg of food was transferred from each of the ten tubes into as many new microtubes where 0.75/1mm of glass beads were previously introduced. One milliliter of MRS broth was added in each microtube and the content was dissolved by using Tissue Lyser II (30 Hz for 1 min). After proper dilutions, 100 µL deriving from each microtube was plated out on MRS agar plates, which were incubated at 37°C for 48h for colonies counting. Finally, 200 µL of sterile glycerol (80%) was added in each microtube to store the bacteria at −80°C. The preparation of the subsequent host generations (G) or diet transfers (T) reflected the described procedure and started from the frozen microtubes obtained in the previous generation. Depending on their bacterial concentration, an adequate number of dilutions was performed in order to inoculate 10^5 CFU/mL to the new Diet and Host tubes for each of the following transfers/generations.

Generation time of *L. plantarum*

Generation time of L. plantarum in the Drosophila experimental setup

To determine the generation time of *L. plantarum* strains in the *Drosophila* Host and Diet experimental setup, we used a modified version of a method that reported the correlation between bacterial growth rate and 16S rRNA content [147]. *L. plantarum* was cultured to stationary phase (18h) and washed in sterile PBS. Serial dilutions have been prepared and 5 µL containing a total of 10^3 colony-forming units (CFUs) were added to 100 µL of GF poor-nutrient diet with and without *Drosophila* larvae (Diet and Host setups, respectively) and kept at 25°C. Samples were snap-frozen in liquid nitrogen at different time points across 5 days of growth. Bacterial RNA was extracted using NucleoSpin RNA Isolation kit

(Macherey-Nagel, Germany) following manufacturer's instructions. Reverse transcription of total extracted RNA into cDNA has been performed using Superscript II (Invitrogen, USA) according to the manufacturer's instructions. Quantitative PCR was performed in a total of 20 µL on a Biorad CFX96 apparatus (Biorad) using SYBR GreenER qPCR Supermix (Invitrogen, USA). The reaction mixture consisted of 0.5 µL of each primer (10 µM each), 12.5 µL of SYBR GreenER mix, 10 µL of water, and 1.5 µL of template cDNA. The PCR conditions included 1 cycle of initial denaturation at 95°C for 2 min, followed by 45 cycles of 95°C for 10 s and 60°C for 40 s. Absolute quantification of 16S rRNA was conducted as follows: five 1:10 serial dilutions of the standard sample (100 ng/µL of cDNA extracted from *L. plantarum*^{NIZO2877} culture) were quantified by real-time PCR using universal 16S primers (forward primer, UniF 5′-GTGSTGCAYG GYTGTCGTCA-3′ and reverse primer, UniR 5′-ACG TCRTCCMCACCTTCCTC-3′) [148]. Each dilution has been tested in triplicate. Melting curves of the detected amplicons were analyzed to ensure specific and unique amplification. Standard curves were generated plotting threshold cycle (Ct) values against the log of the standard sample amount. Based on the data obtained from the standard curve, the Ct values of the Host and Diet samples have been used to obtain the log of their 16S rRNA concentration at each time point. The 16S rRNA values during exponential phase have been used to infer the bacterial generation time following the equation reported by Widdel et al. [149].

Generation time of L. plantarum in the mouse experimental setup

Generation time of *L. plantarum* in the mouse intestine was estimated in the jejunal loops of germ-free mice. *L. plantarum* was grown overnight in MRS broth at 37°C, centrifuged (4500rpm × 10 min), washed with sterile PBS and adjusted to 10^7 CFU/mL. Four 8-week-old germ-free female C57Bl6 mice were anesthetized by intraperitoneal injection of ketamine/xylazine mixture. Mice were shaved on the abdomen, laparotomy was performed, and 2 jejunal loops were created with nylon ligatures. 10^6 CFU of *L. plantarum* in total volume of 100 µL was applied directly into the loops using gauge needle. Intestines with loops were put back inside the abdominal cavity; mice were placed into individual boxes on heated pad (37°C) saturated with 0.5% isofluoran. Mice were euthanized at T0 (immediate loops harvest), T1 (1 h), and T2 (2 h); loops were taken out from the re-opened cavity; and each loop was homogenized in 1 mL sterile PBS using TissueLyser LT (Qiagen) and stainless-steel beads. Serial dilutions in PBS were plated on MRS agar and colonies were counted after 48 h at 37 °C. 10^7 CFU/ml of *L. plantarum* in PBS and the same aliquot after incubation for 2 h at 37 °C were plated out as controls (Additional file 7: Fig. S7). The experiments were approved by the Animal Care Committee of the Czech Academy of Sciences (protocol n. 18/2019) and were in accordance with the EU and NIH Guide for the Care and Use of Laboratory Animals.

L. plantarum generation time in the mouse intestine and diet was estimated by the following formula (as reported by Kushkevych et al. [150]):

$$LpG - Time = \log\ 2 \cdot \frac{t_2 - t_1}{\log X_2 - \log\ X_1}$$
$$(t = \text{time}; X = \text{colony} - \text{forming units per milliliter})$$

Lp^{NIZO2877} serial passages in MRS broth and MRS broth + 0.3 % bile acids (BA)

The ancestral strain *Lp*^{NIZO2877} was cultured overnight at 37°C in 10 mL of MRS broth and MRS broth added with 0.3% sterilized bovine bile acids (Sigma) by using three replicates per condition. On the following day, 100 µL of the overnight culture were plated out on MRS agar plates or MRS agar plates containing 0.3% of sterile bile acids and incubated at 37°C for 48 h for colony counting. At the same time, 10 µL of the overnight culture were transferred into a new MRS broth or MRS broth + 0.3% bile acid medium. The same procedure has been followed for 7 days, thus allowing to determine the bacterial growth (CFU/mL) overtime.

Spectrophotometer assays

Spectrophotometer assays were carried out in the presence of MRS broth or MRS broth added with 0.3% bile acids to investigate the bacterial growth by mimicking the stress conditions found in the mouse gastrointestinal tract. One hundred microliters from the −80°C stock of each strain were cultured on MRS agar plates at 37°C for 48 h. Next, one colony was resuspended in 60 µL of PBS and 10 µL was then tested in triplicates in a 96-well plate containing 100 µL of MRS broth (control), or MRS broth with the addition of 0.3% sterilized bovine bile acids (Sigma), respectively. The bacterial growth was assessed turbidimetrically by measuring optical density at 600 nm every 5 min for 24 h using the Multiskan™ GO Microplate Spectrophotometer (Thermo Scientific).

Electron microscopy

Bacterial colonies transferred from cellophane into cacodylate or phosphate buffer (pH 7.2–7.4) were carefully resuspended and fixed in buffered 3% glutaraldehyde overnight at 4 °C. Thoroughly washed cells were sedimented onto poly-L-lysine coated round 12-mm coverslips for 48 h at 4 °C. Coverslips were then washed with ddH_2O and postfixed in 1% OsO4 at room temperature for 1 h. After

post-fixation, the coverslips were washed three times with ddH_2O and dehydrated in graded alcohol series (25, 50, 75, 90, 96, 100, and 100%), followed with 100% acetone, each step for 20 min. Finally, the coverslips were critical-point dried (K850, Quorum Technologies Ltd, Ringmer, UK) and sputter-coated with 3 nm of platinum (Q150T ES, Quorum Technologies Ltd, Ringmer, UK). Alternatively, pieces of cellophane with bacterial colonies were mounted onto glass slides with Scotch tape. The mounts were then put into a Petri dish with a small container filled with 2% OsO_4 in ddH_2O. Fixation in osmium vapor was then performed in closed Petri dishes in the desiccator for several days at room temperature. Pieces of cellophane with fixed colonies were mounted onto standard aluminum stubs and sputter-coated with 3 nm of platinum (Q150T ES, Quorum Technologies Ltd, Ringmer, UK). All samples were examined in an FEI Nova NanoSEM scanning electron microscope (FEI, Brno, Czech Republic) at 3 to 5 kV using ETD, CBS, and TLD detectors.

Adaptation of *L. plantarum* to the mouse intestine

Three C57Bl6 mice (2 month-old) were colonized with a single dose (2×10^8 CFU/200 µL PBS) of the $Lp^{NIZO2877}$ ancestral strain and $Lp^{NIZO2877}$-derived population evolved in the mouse intestine (sample: F0-10 months) by intragastric gavage. Fecal pellets were sampled every 12 h (until 72 h after gavage) and immediately freezed at −80°C. Bacterial DNA was extracted from mice stool using NucleoSpin DNA Isolation kit (740472.50 Macherey-Nagel, Germany) following manufacturer's instructions. Real-time PCR amplifications were performed on a LightCycler 480 thermal cycler (Roche Diagnostic, Mannheim, Germany) in a final volume of 10 µL, which included 2.5 µL of DNA. The PowerUp™ SYBR™ Green Master Mix (Applied Biosystems™, USA) was used together with 0.25 µL of each primer. Primers designed on *L. plantarum ackA* gene were used to specifically amplify *L. plantarum* DNA, while universal 16S primers were used to amplify the total bacterial DNA (Additional file 16: Table S9). The cycling conditions were as follows: 50 °C for 2 min, followed by 2 min at 95 °C, and 45 cycles at 95 °C for 10 s and 60°C for 1 min. Outputs of real-time amplifications were analyzed by means of the LightCycler 480 Basic Software Version 1.2 (Roche Diagnostic, Mannheim, Germany). The amount of *L. plantarum* DNA detected was normalized to the total bacterial DNA values to account for DNA extraction efficiency according to cycle threshold analysis (ΔC_T).

Fitness assessment of *L. plantarum*-evolved populations in *Drosophila* Host and Diet setups

Lp Host- and Diet-evolved populations belonging to *Drosophila* generation/transfer17 were tested. Ten independent replicate populations (Host: five replicates, Diet: five replicates) were analyzed. Specifically, 10^4 CFU/mL of bacteria taken from each *Lp*-evolved population were inoculated into new microtubes ($N = 10$ microtubes per evolutionary background) containing 250 µL of *Drosophila* food. One-day-old *Drosophila* larvae were added to five out of the 10 microtubes (Host setup). The remaining five microtubes, which included only the fly diet, represented the Diet setup. After 11 days of growth at 25°C, the whole content was transferred from each sample into novel microtubes where 0.75/1mm of glass beads and 1 mL of MRS broth were previously introduced and the content was dissolved by using Tissue Lyser II (30 Hz for 1 min). After proper dilutions, 100 µL from each microtube was plated out on MRS agar plates and cultured at 37°C for 48 h for colony counting.

DNA extraction and whole-genome sequencing

The bacterial samples processed for whole genome sequencing are listened in Additional file 1: Table S1. For the bacterial populations evolved in the mouse intestine, fecal pellets pooled from 3–4 mice were analyzed per time point. For the DNA extraction, 100 µL of each bacterial population or strain has been plated out in two MRS agar plates and incubated for 48 h at 37°C. Genomic DNA was extracted from a mixture of > 1000 colonies per sample by using the Power Soil DNA extraction Kit (Qiagen) by following manufacturer's instructions. DNA library construction and sequencing were carried out by the EMBL Genomics Core Facilities (Heidelberg, Germany). Each sample was pair-end sequenced on an Illumina MiSeq Benchtop Sequencer. Standard procedures produced data sets of Illumina paired-end 250-bp read pairs.

Mutation identification

Raw reads were trimmed and filtered using the parameter SLIDINGWINDOW in Trimmomatic [151], with a 4-base wide sliding window and cutting when the average quality per base drops below 20. The mean coverage per population was between 124 and 193. Processed reads were aligned and analyzed against their respective reference strain (ancestor) genome ($Lp^{NIZO2877}$) (accession number LKHZ01000000). Candidate mutations were identified by running two passes of the *breseq* pipeline in polymorphism mode [152]. Initially, each sample was analyzed individually. Mutation predictions that passed default filtering cutoffs in any one sample were merged into one overall list of candidates. Then, *breseq* was rerun a second time on each sample with the combined list as a user input file so that it output the counts of reads supporting the mutant and reference alleles for each mutation in all samples, even when a potential mutation was at a low frequency or did not

pass other default filtering thresholds in a given sample. We further filtered this list of candidate mutations using a combination of Python and R scripts to remove false-positive calls, including those caused by reads that were mapped incorrectly due to incomplete assembly of the reference genome, and to distinguish low-frequency mutations from sequencing errors. For each candidate mutation, we first examined a Poisson model of the counts of reads supporting the mutant allele with the total counts of reads supporting either the mutant allele or the reference allele in each sample as an offset. Real mutations that are sweeping through populations should have frequencies that significantly deviate in some samples from the average rate across all samples. To test for this signal, we used a likelihood ratio test to calculate the p value for the significance of adding sample as a fixed factor to the Poisson model for each mutation. Candidate mutations with p values that were not significant after correcting for multiple testing using the Benjamini-Hochberg procedure with a false-discovery rate of 1% were removed. We next eliminated candidate mutations with frequencies that were ≥5% in at least half the samples from all treatments. Then, we kept only mutations that had a >20% range in their predicted frequencies among the samples in a given evolution treatment or that both reached a frequency of >10% and appeared in less than or equal to half of these samples to arrive at the final lists of mutations that were analyzed.

Mutation accumulation rates and spectra

We fit linear models to the summed frequencies of all mutations observed in each sample to estimate average rates of mutation accumulation per generation. These models were constrained to have no initial mutations (i.e., an intercept term of zero). For the fly diet, fly host, and mouse diet treatments, we fit models with one rate of mutation accumulation. For the mouse host treatment, we fit three rates: one for ancestral (nonmutator) lineages, one for *mutS* A41T lineages, and one for *mutS* Δ1303 lineages. We modeled the total mutation frequency in a sample as the sum of each of these three population's rates multiplied by its frequency in the population and the number of generations that had elapsed from the beginning of the experiment up to that sample. This procedure assumes that both mutator lineages evolved close to the beginning of the experiment and experienced one constant rate of mutation accumulation throughout their history. The frequencies of the two *mutS* alleles in each sample were used to estimate the fraction of the population in each of the three categories. The *mutS* lineage frequencies were normalized to a total of 100% when they slightly exceeded this value when added together due to experimental and/or sampling errors in the estimates of allele frequencies from sequencing reads.

Muller plots

We included only mutations that reached at least a 10% frequency in a population when constructing Muller plots. Three mutations associated with tRNA and rRNA genes that met this criterion were excluded because they appeared to result from a single structural variant that could not be fully resolved to ensure that the inferred mutation frequencies were accurate. Since whole-population (metagenomic) sequencing does not provide information about linkage between mutations, we inferred which mutations were likely in the same genetic backgrounds from how their frequencies changed over time under the assumption that there was no recombination during the experiment (i.e., purely asexual reproduction). We also assumed that once a lineage had a mutation in a certain gene that it was unlikely to sustain a second mutation in the same gene since these populations retained the low ancestral mutation rate. These rules disambiguated how most mutations could be ordered. We then corrected the genotype frequencies observed at each time point for two types of errors resulting from how the frequencies of all mutations in a sample are estimated independently from the sequencing reads overlapping each genomic site. First, we reduced the frequencies of genotypes with new mutations that exceeded the frequencies of their ancestral genotypes to fit within the earlier group. Second, we normalized the total frequencies of all genotypes at a given time point to 100% if it exceeded this value. Both types of corrections changed the inferred genotype frequencies by <10% in all cases. We used the ggmuller R package to plot the resulting dynamics and then manually adjusted the locations of the curves between the time points with measured values to improve the visibility of mutations and lineages.

Data analysis

Data representation and statistical analyses were performed using GraphPad PRISM 9 software (GraphPad software, www.graphpad.com). All the pairwise comparison were performed by using the unpaired t-test ($^{*}p \leq 0.05$, $^{**}p<0.01$, $^{***}p<0.001$; degree of freedom – df = total sample size minus 2). ANCOVA test between *Lp* Host and Diet growth trend of *Drosophila* setup has been performed using the sm-ancova package (version 2.2-5.7.1) on R Studio software (RStudio Team, www.rstudio.com) (significance p <0.05; $^{*}p<0.05$, $^{**}p<0.01$, $^{***}p<0.001$). Predicted gene functional categories have been determined according to their COG group with EggNOG v.5.1 [153].

Supplementary Information

The online version contains supplementary material available at https://doi.org/10.1186/s12915-022-01477-y.

Additional file 1: Figure S1. A Macroscopical appearance of smooth/rough morphotypes isolated during Lp evolution in the mouse intestine. B, C Microscopical appearance of smooth/rough Lp morphotypes at the electron microscope. d Relative abundance of smooth and rough Lp morphotypes observed at mice generations 0 (F0) and 3 (F3). Lines above each bar indicate the standard error of the mean (SEM) determined by considering three replicates for each generation.

Additional file 2: Figure S2. *Lp*^{NIZO2877}growth monitored during serial Transfers (T) in MRS broth and MRS broth added to with 0.3% bile acid (BA). At each transfer, the three circles represent the growth obtained from each of the three experimental replicates. Asterisks refer to statistical comparison between bacterial CFUs obtained from the two experimental conditions at each transfer (unpaired t-test; *** $p < 0.001$; df = 4).

Additional file 3: Figure S3. Growth curves of the Lp strains under standard growth conditions (MRS broth) and in MRS broth added to with 0.3% bile acid (BA). Each curve represents the mean of at least three replicates.

Additional file 4: Figure S4. Standard growth curves of the *Lp* strains cultured in MRS broth and MRS broth + 0.3% bile acid (BA). The strains tested include (A) the *Lp*^{NIZO2877}ancestor; (B, C) Smooth and Rough colonies isolated from mice generation 0; (D, E) Smooth and rough colonies isolated from mice generation 3; (F, G) Smooth and Rough colonies isolated from the Diet setup.

Additional file 5: Figure S5. Total Manhattan distances between the frequencies of different mutations and the *mutS* A41T and *mutS* Δ1303 alleles over all samples from the mouse evolution experiment were used to classify mutations as occurring in each hypermutator lineage for examining the base substitution spectra. Mutations with distances < 0.4 to both lineages rose to a high frequency along with each *mutS* mutation. The cluster of mutations at a distance of ~1.0 from *mutS* A41T swept within this lineage later in the experiment.

Additional file 6: Figure S6. Bold full lines indicate Lp^{NIZO2877}growth monitored after 7 (A) and 11 days (B) of incubation in the presence (Host setup) or absence (Diet setup) of Drosophila. Lighter full lines indicate the re-monitoring of Lp growth from Generations/Transfers 6 to 12. ANCOVA (* $p < 0.01$, ** $p < 0.001$, and *** $p < 0.0001$).

Additional file 7: Figure S7. *L. plantarum* loads retrieved in the jejunal loops of germ-free mice. Bars indicate the standard error of the mean (SEM).

Additional file 8: Table S1. List of *Lp*^{NIZO2877}-evolved populations sequenced in this study.

Additional file 9: Table S2. List of all mutations detected in the genomes of the *L. plantarum* populations evolved in the mouse diet.

Additional file 10: Table S3. List of all mutations detected in the genomes of the *L. plantarum*-evolved colonies (Rough and Smooth morphologies) isolated from the mouse diet (Transfer 14, replicate 2).

Additional file 11: Table S4. List of all mutations detected in the genomes of the *L. plantarum* populations evolved in the mouse intestine.

Additional file 12: Table S5. List of mutations detected in the genomes of the *L. plantarum* populations evolved in the second replicate of *L. plantarum* experimental evolution in the mouse intestine. Mutations identified by Sanger sequencing were confirmed from alignments of both forward and reverse reads.

Additional file 13: Table S6. *Lp*^{NIZO2877}-mutated genes persisting over the course of the experimental evolution in the mouse intestine. The targets were chosen by selecting mutated genes that persisted in at least seven Host-evolved *Lp* populations. Predicted functional categories have been determined according to their COG group with EggNOG v.5.1.

Additional file 14: Table S7. List of all mutations detected in the genomes of the *L. plantarum* populations evolved in the fly diet.

Additional file 15: Table S8. List of all mutations detected in the genomes of the *L. plantarum* populations evolved in the fly host setup.

Additional file 16: Table S9. Primer sequences.

Acknowledgements
We would like to thank Jaroslava Valerová and Šárka Maisnerová for excellent technical assistance. The authors acknowledge the Texas Advanced Computing Center (TACC) at The University of Texas at Austin for providing high-performance computing resources.

Authors' contributions
M.E.M. and M.S. designed the research; E.M., M.G, D.S., A.J., O.B., O.K., N.S., T.H., and M.S. performed the research; E.M., I.G., J.B., M.S., and M.E.M. analyzed the data; and E.M., M.S., and M.E.M. wrote the paper. The authors read and approved the final manuscript.

Funding
Research in the MEM lab was supported by the STARS@UNIPD Funding Programme (Starting Grant 2017) of the University of Padova and by the Visiting Programme 2018 grant from Fondazione Cassa di Risparmio di Padua e Rovigo (CARIPARO Foundation). MS lab was supported by the Czech Science Foundation JUNIOR STAR grant (GAČR 21-19640M) and Ministry of Education, Youth and Sports of the Czech Republic (EMBO Installation Grant 4139). JEB lab was supported by the Welch Foundation (F-1979-20190330), the US National Science Foundation (DEB-1813069), and the US Army Research Office (W911NF-20-1-0195).

Availability of data and materials
All data needed to evaluate the conclusions in the paper are present in the paper, the Supplementary Information files, and/or publicly available repositories. All bacterial populations' genomes sequenced in this work were deposited at NCBI and are publicly accessible at https://www.ncbi.nlm.nih.gov/bioproject/PRJNA808881 [154].

Declarations

Ethics approval and consent to participate
Not applicable.

Consent for publication
Not applicable.

Competing interests
The authors declare that they have no competing interests.

Author details
[1]Department of Comparative Biomedicine and Food Science, University of Padua, Padua, Italy. [2]Laboratory of Gnotobiology, Institute of Microbiology of the Czech Academy of Sciences, Novy Hradek, Czech Republic. [3]Laboratory of Molecular Structure Characterization, Institute of Microbiology of the Czech Academy of Sciences, Prague, Czech Republic. [4]Department of Molecular Biosciences, The University of Texas at Austin, Austin, TX, USA.

Received: 13 September 2022 Accepted: 23 November 2022
Published online: 27 December 2022

References
1. Dethlefsen L, McFall-Ngai M, Relman DA. An ecological and evolutionary perspective on human–microbe mutualism and disease. Nature. 2007;449:811–8.
2. Hooper LV, Midtvedt T, Gordon JI. How host-microbial interactions shape the nutrient environment of the mammalian intestine. Annu Rev Nutr. 2002;22:283–307.
3. Ley RE, Peterson DA, Gordon JI. Ecological and evolutionary forces shaping microbial diversity in the human intestine. Cell. 2006;124:837–48.

4. Moeller AH, Caro-Quintero A, Mjungu D, Georgiev AV, Lonsdorf EV, Muller MN, et al. Cospeciation of gut microbiota with hominids. Science. 2016;353:380–2.
5. Backhed F. Host-bacterial mutualism in the human intestine. Science. 2005;307:1915–20.
6. Ley RE, Hamady M, Lozupone C, Turnbaugh PJ, Ramey RR, Bircher JS, et al. Evolution of mammals and their gut microbes. Science. 2008;320:1647–51.
7. Gill SR, Pop M, DeBoy RT, Eckburg PB, Turnbaugh PJ, Samuel BS, et al. Metagenomic analysis of the human distal gut microbiome. Science. 2006;312:1355–9.
8. Nicholson JK, Holmes E, Kinross J, Burcelin R, Gibson G, Jia W, et al. Host-gut microbiota metabolic interactions. Science. 2012;336:1262–7.
9. Schwarzer M, Strigini M, Leulier F. Gut microbiota and host juvenile growth. Calcif Tissue Int. 2018;102:387–405.
10. Storelli G, Defaye A, Erkosar B, Hols P, Royet J, Leulier F. Lactobacillus plantarum promotes Drosophila systemic growth by modulating hormonal signals through TOR-dependent nutrient sensing. Cell Metab. 2011;14:403–14.
11. Sjögren K, Engdahl C, Henning P, Lerner UH, Tremaroli V, Lagerquist MK, et al. The gut microbiota regulates bone mass in mice. J Bone Miner Res. 2012;27:1357–67.
12. Bouskra D, Brézillon C, Bérard M, Werts C, Varona R, Boneca IG, et al. Lymphoid tissue genesis induced by commensals through NOD1 regulates intestinal homeostasis. Nature. 2008;456:507–10.
13. Hooper LV, Littman DR, Macpherson AJ. Interactions between the microbiota and the immune system. Science. 2012;336:1268–73.
14. Mazmanian SK, Liu CH, Tzianabos AO, Kasper DL. An immunomodulatory molecule of symbiotic bacteria directs maturation of the host immune system. Cell. 2005;122:107–18.
15. Garrett WS, Gordon JI, Glimcher LH. Homeostasis and inflammation in the intestine. Cell. 2010;140:859–70.
16. van de Wouw M, Schellekens H, Dinan TG, Cryan JF. Microbiota-gut-brain axis: modulator of host metabolism and appetite. J Nutr. 2017;147:727–45.
17. Bocci V. The neglected organ: bacterial flora has a crucial immunostimulatory role. Perspect Biol Med. 1992;35:251–60.
18. O'Hara AM, Shanahan F. The gut flora as a forgotten organ. EMBO Rep. 2006;7:688–93.
19. Qin J, Li R, Raes J, Arumugam M, Burgdorf KS, et al. A human gut microbial gene catalogue established by metagenomic sequencing. Nature. 2010;464:59–65.
20. Blum JE, Fischer CN, Miles J, Handelsman J. Frequent replenishment sustains the beneficial microbiome of Drosophila melanogaster. mBio. 2013;4:e00860–13.
21. Broderick NA, Buchon N, Lemaitre B. Microbiota-induced changes in Drosophila melanogaster host gene expression and gut morphology. mBio. 2014;5:e01117–4.
22. Chandler JA, Morgan Lang J, Bhatnagar S, Eisen JA, Kopp A. Bacterial communities of diverse Drosophila species: ecological context of a host–microbe model system. PLoS Genet. 2011;7:e1002272.
23. Douglas AE. Lessons from Studying Insect Symbioses. Cell Host Microbe. 2011;10:359–67.
24. Early AM, Shanmugarajah N, Buchon N, Clark AG. Drosophila genotype influences commensal bacterial levels. PLoS One. 2017;12:e0170332.
25. Staubach F, Baines JF, Künzel S, Bik EM, Petrov DA. Host species and environmental effects on bacterial communities associated with Drosophila in the laboratory and in the natural environment. PLoS One. 2013;8:e70749.
26. Storelli G, Strigini M, Grenier T, Bozonnet L, Schwarzer M, Daniel C, et al. Drosophila perpetuates nutritional mutualism by promoting the fitness of its intestinal symbiont Lactobacillus plantarum. Cell Metab. 2018;27:362–377.e8.
27. Wong AC-N, Dobson AJ, Douglas AE. Gut microbiota dictates the metabolic response of *Drosophila* to diet. J Exp Biol. 2014;217:1894–901.
28. Wong CNA, Ng P, Douglas AE. Low-diversity bacterial community in the gut of the fruitfly Drosophila melanogaster: bacterial community in Drosophila melanogaster. Environ Microbiol. 2011;13:1889–900.
29. Wong AC-N, Chaston JM, Douglas AE. The inconstant gut microbiota of Drosophila species revealed by 16S rRNA gene analysis. ISME J. 2013;7:1922–32.
30. Aagaard K, Ma J, Antony KM, Ganu R, Petrosino J, Versalovic J. The placenta harbors a unique microbiome. Sci Transl Med. 2014;6:237ra65.
31. Engel P, Moran NA. The gut microbiota of insects – diversity in structure and function. FEMS Microbiol Rev. 2013;37:699–735.
32. Faith JJ, Guruge JL, Charbonneau M, Subramanian S, Seedorf H, Goodman AL, et al. The long-term stability of the human gut microbiota. Science. 2013;341:1237439.
33. Lee SM, Donaldson GP, Mikulski Z, Boyajian S, Ley K, Mazmanian SK. Bacterial colonization factors control specificity and stability of the gut microbiota. Nature. 2013;501:426–9.
34. Perez-Muñoz ME, Arrieta M-C, Ramer-Tait AE, Walter J. A critical assessment of the "sterile womb" and "in utero colonization" hypotheses: implications for research on the pioneer infant microbiome. Microbiome. 2017;5:48.
35. Koenig JE, Spor A, Scalfone N, Fricker AD, Stombaugh J, Knight R, et al. Succession of microbial consortia in the developing infant gut microbiome. Proc Natl Acad Sci. 2011;108 Supplement_1:4578–85.
36. Palmer C, Bik EM, DiGiulio DB, Relman DA, Brown PO. Development of the human infant intestinal microbiota. PLoS Biol. 2007;5:e177.
37. Candela M, Biagi E, Maccaferri S, Turroni S, Brigidi P. Intestinal microbiota is a plastic factor responding to environmental changes. Trends Microbiol. 2012;20:385–91.
38. Flores GE, Caporaso JG, Henley JB, Rideout JR, Domogala D, Chase J, et al. Temporal variability is a personalized feature of the human microbiome. Genome Biol. 2014;15:531.
39. Rawls JF, Mahowald MA, Ley RE, Gordon JI. Reciprocal gut microbiota transplants from zebrafish and mice to germ-free recipients reveal host habitat selection. Cell. 2006;127:423–33.
40. Walker AW, Ince J, Duncan SH, Webster LM, Holtrop G, Ze X, et al. Dominant and diet-responsive groups of bacteria within the human colonic microbiota. ISME J. 2011;5:220–30.
41. Benson AK. The gut microbiome—an emerging complex trait. Nat Genet. 2016;48:1301–2.
42. Falony G, Joossens M, Vieira-Silva S, Wang J, Darzi Y, Faust K, et al. Population-level analysis of gut microbiome variation. 2016.
43. Goodrich JK, Davenport ER, Beaumont M, Jackson MA, Knight R, Ober C, et al. Genetic determinants of the gut microbiome in UK twins. Cell Host Microbe. 2016;19:731–43.
44. Goodrich JK, Waters JL, Poole AC, Sutter JL, Koren O, Blekhman R, et al. Human genetics shape the gut microbiome. Cell. 2014;159:789–99.
45. McKnite AM, Perez-Munoz ME, Lu L, Williams EG, Brewer S, Andreux PA, et al. Murine gut microbiota is defined by host genetics and modulates variation of metabolic traits. PLoS One. 2012;7:e39191.
46. Srinivas G, Möller S, Wang J, Künzel S, Zillikens D, Baines JF, et al. Genome-wide mapping of gene–microbiota interactions in susceptibility to autoimmune skin blistering. Nat Commun. 2013;4:2462.
47. Turnbaugh PJ, Ridaura VK, Faith JJ, Rey FE, Knight R, Gordon JI. The effect of diet on the human gut microbiome: a metagenomic analysis in humanized gnotobiotic mice. Sci Transl Med. 2009;1:6ra14-6ra14.
48. Sousa A, Frazão N, Ramiro RS, Gordo I. Evolution of commensal bacteria in the intestinal tract of mice. Curr Opin Microbiol. 2017;38:114–21.
49. Johansson MEV, Phillipson M, Petersson J, Velcich A, Holm L, Hansson GC. The inner of the two Muc2 mucin-dependent mucus layers in colon is devoid of bacteria. Proc Natl Acad Sci U S A. 2008;105:15064–9.
50. Salzman NH, Hung K, Haribhai D, Chu H, Karlsson-Sjöberg J, Amir E, et al. Enteric defensins are essential regulators of intestinal microbial ecology. Nat Immunol. 2010;11:76–82.
51. Vaishnava S, Yamamoto M, Severson KM, Ruhn KA, Yu X, Koren O, et al. The antibacterial lectin RegIII promotes the spatial segregation of microbiota and host in the intestine. Science. 2011;334:255–8.
52. Macpherson AJ, Geuking MB, McCoy KD. Immune responses that adapt the intestinal mucosa to commensal intestinal bacteria. Immunology. 2005;115:153–62.
53. Imhann F, Bonder MJ, Vich Vila A, Fu J, Mujagic Z, Vork L, et al. Proton pump inhibitors affect the gut microbiome. Gut. 2016;65:740–8.
54. Jackson MA, Goodrich JK, Maxan M-E, Freedberg DE, Abrams JA, Poole AC, et al. Proton pump inhibitors alter the composition of the gut microbiota. Gut. 2016;65:749–56.
55. O'May GA, Reynolds N, Smith AR, Kennedy A, Macfarlane GT. Effect of pH and antibiotics on microbial overgrowth in the stomachs and

duodena of patients undergoing percutaneous endoscopic gastrostomy feeding. J Clin Microbiol. 2005;43:3059–65.
56. Cho I, Yamanishi S, Cox L, Methé BA, Zavadil J, Li K, et al. Antibiotics in early life alter the murine colonic microbiome and adiposity. Nature. 2012;488:621–6.
57. Forslund K. Disentangling type 2 diabetes and metformin treatment signatures in the human gut microbiota. 2015; 13.
58. Vich Vila A, Collij V, Sanna S, Sinha T, Imhann F, Bourgonje AR, et al. Impact of commonly used drugs on the composition and metabolic function of the gut microbiota. Nat Commun. 2020;11:362.
59. Zhernakova A, Kurilshikov A, Bonder MJ, Tigchelaar EF, Schirmer M, Vatanen T, et al. Population-based metagenomics analysis reveals markers for gut microbiome composition and diversity. Science. 2016;352:565–9.
60. Penders J, Thijs C, Vink C, Stelma FF, Snijders B, Kummeling I, et al. Factors influencing the composition of the intestinal microbiota in early infancy. Pediatrics. 2006;118:511–21.
61. Dominguez-Bello MG, Blaser MJ, Ley RE, Knight R. Development of the human gastrointestinal microbiota and insights from high-throughput sequencing. Gastroenterology. 2011;140:1713–9.
62. Zivkovic AM, German JB, Lebrilla CB, Mills DA. Human milk glycobiome and its impact on the infant gastrointestinal microbiota. Proc Natl Acad Sci. 2011;108 Supplement_1:4653–8.
63. Karl JP, Margolis LM, Madslien EH, Murphy NE, Castellani JW, Gundersen Y, et al. Changes in intestinal microbiota composition and metabolism coincide with increased intestinal permeability in young adults under prolonged physiological stress. Am J Physiol Gastrointest Liver Physiol. 2017;312:G559–71.
64. David LA, Maurice CF, Carmody RN, Gootenberg DB, Button JE, Wolfe BE, et al. Diet rapidly and reproducibly alters the human gut microbiome. Nature. 2014;505:559–63.
65. Erkosar B, Storelli G, Defaye A, Leulier F. Host-intestinal microbiota mutualism: "learning on the fly". Cell Host Microbe. 2013;13:8–14.
66. Jehrke L, Stewart FA, Droste A, Beller M. The impact of genome variation and diet on the metabolic phenotype and microbiome composition of Drosophila melanogaster. Sci Rep. 2018;8:6215.
67. Obadia B, Keebaugh ES, Yamada R, Ludington WB, Ja WW. Diet influences host–microbiota associations in *Drosophila*. Proc Natl Acad Sci U S A. 2018;115:E4547–8.
68. Hildebrandt MA, Hoffmann C, Sherrill-Mix SA, Keilbaugh SA, Hamady M, Chen Y, et al. High-fat diet determines the composition of the murine gut microbiome independently of obesity. Gastroenterology. 2009;137:1716–1724.e2.
69. Muegge BD, Kuczynski J, Knights D, Clemente JC, Gonzalez A, Fontana L, et al. Diet drives convergence in gut microbiome functions across mammalian phylogeny and within humans. Science. 2011;332:970–4.
70. Ridaura VK, Faith JJ, Rey FE, Cheng J, Duncan AE, Kau AL, et al. Gut microbiota from twins discordant for obesity modulate metabolism in mice. Science. 2013;341:1241214.
71. Rothschild D, Weissbrod O, Barkan E, Kurilshikov A, Korem T, Zeevi D, et al. Environment dominates over host genetics in shaping human gut microbiota. Nature. 2018;555:210–5.
72. Sonnenburg ED, Smits SA, Tikhonov M, Higginbottom SK, Wingreen NS, Sonnenburg JL. Diet-induced extinctions in the gut microbiota compound over generations. Nature. 2016;529:212–5.
73. Wu GD, Chen J, Hoffmann C, Bittinger K, Chen Y-Y, Keilbaugh SA, et al. Linking long-term dietary patterns with gut microbial enterotypes. Science. 2011;334:105–8.
74. Desai MS, Seekatz AM, Koropatkin NM, Kamada N, Hickey CA, Wolter M, et al. A dietary fiber-deprived gut microbiota degrades the colonic mucus barrier and enhances pathogen susceptibility. Cell. 2016;167:1339–1353.e21.
75. Barreto HC. The landscape of adaptive evolution of a gut commensal bacteria in aging mice; 2019.
76. Barreto HC, Frazão N, Sousa A, Konrad A, Gordo I. Mutation accumulation and horizontal gene transfer in *Escherichia coli* colonizing the gut of old mice. Commun Integr Biol. 2020;13:89–96.
77. Barroso-Batista J, Sousa A, Lourenço M, Bergman M-L, Sobral D, Demengeot J, et al. The first steps of adaptation of Escherichia coli to the gut are dominated by soft sweeps. PLoS Genet. 2014;10:e1004182.
78. Yilmaz B, Mooser C, Keller I, Li H, Zimmermann J, Bosshard L, et al. Long-term evolution and short-term adaptation of microbiota strains and sub-strains in mice. Cell Host Microbe. 2021;29:650–63.
79. Fabich AJ, Leatham MP, Grissom JE, Wiley G, Lai H, Najar F, et al. Genotype and phenotypes of an intestine-adapted Escherichia coli K-12 mutant selected by animal passage for superior colonization. Infect Immun. 2011;79:2430–9.
80. Giraud A, Arous S, Paepe MD, Gaboriau-Routhiau V, Bambou J-C, Rakotobe S, et al. Dissecting the genetic components of adaptation of Escherichia coli to the mouse gut. PLoS Genet. 2008;4:e2.
81. Lescat M, Launay A, Ghalayini M, Magnan M, Glodt J, Pintard C, et al. Using long-term experimental evolution to uncover the patterns and determinants of molecular evolution of an *Escherichia coli* natural isolate in the streptomycin-treated mouse gut. Mol Ecol. 2017;26:1802–17.
82. Paepe MD, Taddei F, Cerf-Bensussan N. Trade-off between bile resistance and nutritional competence drives Escherichia coli diversification in the mouse gut. PLoS Genet. 2011;7:13.
83. Ramiro RS, Durão P, Bank C, Gordo I. Low mutational load and high mutation rate variation in gut commensal bacteria. PLoS Biol. 2020;18:e3000617.
84. Dapa T, Ramiro RS, Pedro MF, Gordo I, Xavier KB. Diet leaves a genetic signature in a keystone member of the gut microbiota. Cell Host Microbe. 2022;30:183–199.e10.
85. Giraud A. Costs and benefits of high mutation rates: adaptive evolution of bacteria in the mouse gut. Science. 2001;291:2606–8.
86. Marco ML, Peters THF, Bongers RS, Molenaar D, van Hemert S, Sonnenburg JL, et al. Lifestyle of Lactobacillus plantarum in the mouse cecum. Environ Microbiol. 2009;11:2747–57.
87. Martino ME, Joncour P, Leenay R, Gervais H, Shah M, Hughes S, et al. Bacterial adaptation to the host's diet is a key evolutionary force shaping Drosophila-Lactobacillus symbiosis. Cell Host Microbe. 2018;24:109–119.e6.
88. Schwarzer M, Makki K, Storelli G, Machuca-Gayet I, Srutkova D, Hermanova P, et al. Lactobacillus plantarum strain maintains growth of infant mice during chronic undernutrition. Science. 2016;351:854–7.
89. Bron PA, Marco M, Hoffer SM, Van Mullekom E, de Vos WM, Kleerebezem M. Genetic characterization of the bile salt response in *Lactobacillus plantarum* and analysis of responsive promoters in vitro and in situ in the gastrointestinal tract. J Bacteriol. 2004;186:7829–35.
90. Gandhi A, Shah NP. Effect of salt stress on morphology and membrane composition of Lactobacillus acidophilus, Lactobacillus casei, and Bifidobacterium bifidum, and their adhesion to human intestinal epithelial-like Caco-2 cells. J Dairy Sci. 2016;99:2594–605.
91. Ingham CJ, Beerthuyzen M, van Hylckama VJ. Population heterogeneity of Lactobacillus plantarum WCFS1 microcolonies in response to and recovery from acid stress. AEM. 2008;74:7750–8.
92. Yang DC, Blair KM, Salama NR. Staying in shape: the impact of cell shape on bacterial survival in diverse environments. Microbiol Mol Biol Rev. 2016;80:187–203.
93. Hussain MA, Hosseini Nezhad M, Sheng Y, Amoafo O. Proteomics and the stressful life of lactobacilli. FEMS Microbiol Lett. 2013;349:1–8.
94. Merritt ME, Donaldson JR. Effect of bile salts on the DNA and membrane integrity of enteric bacteria. J Med Microbiol. 2009;58:1533–41.
95. Sistrunk JR, Nickerson KP, Chanin RB, Rasko DA, Faherty CS. Survival of the fittest: how bacterial pathogens utilize bile to enhance infection. Clin Microbiol Rev. 2016;29:819–36.
96. Urdaneta V, Casadesús J. Interactions between bacteria and bile salts in the gastrointestinal and hepatobiliary tracts. Front Med. 2017;4:163.
97. Schaaper RM, Dunn RL. Spectra of spontaneous mutations in Escherichia coli strains defective in mismatch correction: the nature of in vivo DNA replication errors. Proc Natl Acad Sci U S A. 1987;84:6220–4.
98. Wagner J, Nohmi T. Escherichia coli DNA polymerase IV mutator activity: genetic requirements and mutational specificity. J Bacteriol. 2000;182:4587–95.
99. Mo J-Y, Maki H, Sekiguchi M. Mutational specificity of the dnaE173 mutator associated with a defect in the catalytic subunit of DNA polymerase III of Escherichia coli. J Mol Biol. 1991;222:925–36.

100. Cen S, Yin R, Mao B, Zhao J, Zhang H, Zhai Q, et al. Comparative genomics shows niche-specific variations of Lactobacillus plantarum strains isolated from human, Drosophila melanogaster, vegetable and dairy sources. Food Biosci. 2020;35:100581.
101. Parker A, Lawson MAE, Vaux L, Pin C. Host-microbe interaction in the gastrointestinal tract. Environ Microbiol. 2018;20:2337–53.
102. Tannock GW. What immunologists should know about bacterial communities of the human bowel. Semin Immunol. 2007;19:94–105.
103. Han S, Lu Y, Xie J, Fei Y, Zheng G, Wang Z, et al. Probiotic gastrointestinal transit and colonization after oral administration: a long journey. Front Cell Infect Microbiol. 2021;11:609722.
104. Louis P, O'Byrne CP. Life in the gut: microbial responses to stress in the gastrointestinal tract. Sci Prog. 2010;93:7–36.
105. Wainwright M. Extreme pleomorphism and the bacterial life cycle: a forgotten controversy. Perspect Biol Med. 1997;40:407–14.
106. Capozzi V, Weidmann S, Fiocco D, Rieu A, Hols P, Guzzo J, et al. Inactivation of a small heat shock protein affects cell morphology and membrane fluidity in Lactobacillus plantarum WCFS1. Res Microbiol. 2011;162:419–25.
107. Kubota H, Senda S, Nomura N, Tokuda H, Uchiyama H. Biofilm formation by lactic acid bacteria and resistance to environmental stress. J Biosci Bioeng. 2008;106:381–6.
108. van Bokhorst-van de Veen H, Abee T, Tempelaars M, Bron PA, Kleerebezem M, Marco ML. Short- and long-term adaptation to ethanol stress and its cross-protective consequences in Lactobacillus plantarum. Appl Environ Microbiol. 2011;77:5247–56.
109. Wei T, Mei L, Wang Z-G, Xue X. Morphological and genetic responses of lactobacillus plantarum FQR to nitrite and its practical applications. J Food Saf. 2017;37:e12327.
110. Pieterse B, Leer RJ, Schuren FHJ, van der Werf MJ. Unravelling the multiple effects of lactic acid stress on Lactobacillus plantarum by transcription profiling. Microbiology. 2005;151:3881–94.
111. Parlindungan E, Dekiwadia C, Tran KTM, Jones OAH, May BK. Morphological and ultrastructural changes in Lactobacillus plantarum B21 as an indicator of nutrient stress. LWT. 2018;92:556–63.
112. Eswaramoorthy P, Erb ML, Gregory JA, Silverman J, Pogliano K, Pogliano J, et al. Cellular architecture mediates DivIVA ultrastructure and regulates Min activity in Bacillus subtilis. mBio. 2011;22;2:e00257–11.
113. Kaval KG, Halbedel S. Architecturally the same, but playing a different game: the diverse species-specific roles of DivIVA proteins. Virulence. 2012;3:406–7.
114. Cha JH, Stewart GC. The divIVA minicell locus of Bacillus subtilis. J Bacteriol. 1997;179:1671–83.
115. Halbedel S, Hahn B, Daniel RA, Flieger A. DivIVA affects secretion of virulence-related autolysins in Listeria monocytogenes: L. monocytogenes DivIVA. Mol Microbiol. 2012;83:821–39.
116. Deutscher J, Francke C, Postma PW. How phosphotransferase system-related protein phosphorylation regulates carbohydrate metabolism in bacteria. Microbiol Mol Biol Rev. 2006;70:939–1031.
117. Zhang X, Top J, de Been M, Bierschenk D, Rogers M, Leendertse M, et al. Identification of a genetic determinant in clinical Enterococcus faecium strains that contributes to intestinal colonization during antibiotic treatment. J Infect Dis. 2013;207:1780–6.
118. Huang S, Jiang S, Huo D, Allaband C, Estaki M, Cantu V, et al. Candidate probiotic Lactiplantibacillus plantarum HNU082 rapidly and convergently evolves within human, mice, and zebrafish gut but differentially influences the resident microbiome. Microbiome. 2021;9:151.
119. Echols H, Goodman MF. Fidelity mechanisms in DNA replication. Annu Rev Biochem. 1991;60:477–511.
120. Fukui K. DNA mismatch repair in eukaryotes and bacteria. J Nucleic Acids. 2010;2010:260512.
121. Tompkins JD, Nelson JL, Hazel JC, Leugers SL, Stumpf JD, Foster PL. Error-prone polymerase, DNA polymerase IV, is responsible for transient hypermutation during adaptive mutation in Escherichia coli. J Bacteriol. 2003;185:3469–72.
122. Horst J. Escherichia coli mutator genes. Trends Microbiol. 1999;7:29–36.
123. Miller JH. Spontaneous mutators in bacteria: insights into pathways of mutagenesis and repair. Annu Rev Microbiol. 1996;50:625–43.
124. Modrich P, Lahue R. Mismatch repair in replication fidelity, genetic recombination, and cancer biology. 1996. https://doi.org/10.1146/annurev.bi.65.070196.000533.
125. Sundin GW, Weigand MR. The microbiology of mutability. FEMS Microbiol Lett. 2007;277:11–20.
126. Denamur E, Matic I. Evolution of mutation rates in bacteria. Mol Microbiol. 2006;60:820–7.
127. Weigand MR, Sundin GW. General and inducible hypermutation facilitate parallel adaptation in Pseudomonas aeruginosa despite divergent mutation spectra. PNAS. 2012;109:13680–5.
128. Tenaillon O, Barrick JE, Ribeck N, Deatherage DE, Blanchard JL, Dasgupta A, et al. Tempo and mode of genome evolution in a 50,000-generation experiment. Nature. 2016;536:165–70.
129. Cox EC, Gibson TC. Selection for high mutation rates in chemostats. Genetics. 1974;77:169–84.
130. Mao EF, Lane L, Lee J, Miller JH. Proliferation of mutators in A cell population. J Bacteriol. 1997;179:417–22.
131. Sniegowski PD, Gerrish PJ, Lenski RE. Evolution of high mutation rates in experimental populations of E. coli. Nature. 1997;387:703–5.
132. Bjedov I, Tenaillon O, Gérard B, Souza V, Denamur E, Radman M, et al. Stress-induced mutagenesis in bacteria. Science. 2003;300:1404–9.
133. Frazão N, Sousa A, Lässig M, Gordo I. Horizontal gene transfer overrides mutation in *Escherichia coli* colonizing the mammalian gut. Proc Natl Acad Sci U S A. 2019;116:17906–15.
134. Zhao S, Lieberman TD, Poyet M, Kauffman KM, Gibbons SM, Groussin M, et al. Adaptive evolution within gut microbiomes of healthy people. Cell Host Microbe. 2019;25:656–667.e8.
135. Weidenmaier C, Kristian S, Peschel A. Bacterial resistance to antimicrobial host defenses - an emerging target for novel antiinfective strategies? CDT. 2003;4:643–9.
136. Lennarz WJ, J.A. N, J R. The participation of srna in the enzymatic synthesis of o-l-lysyl phosphatidylgylcerol in Staphylococcus aureus. Proc Natl Acad Sci U S A. 1966;55:934–41.
137. Staubitz P, Neumann H, Schneider T, Wiedemann I, Peschel A. MprF-mediated biosynthesis of lysylphosphatidylglycerol, an important determinant in staphylococcal defensin resistance. FEMS Microbiol Lett. 2004;231:67–71.
138. Peschel A, Jack RW, Otto M, Collins LV, Staubitz P, Nicholson G, et al. Staphylococcus aureus resistance to human defensins and evasion of neutrophil killing via the novel virulence factor Mprf is based on modification of membrane lipids with l-lysine. J Exp Med. 2001;193:1067–76.
139. Samant S, Hsu F-F, Neyfakh AA, Lee H. The *Bacillus anthracis* protein MprF is required for synthesis of lysylphosphatidylglycerols and for resistance to cationic antimicrobial peptides. J Bacteriol. 2009;191:1311–9.
140. Sohlenkamp C, Galindo-Lagunas KA, Guan Z, Vinuesa P, Robinson S, Thomas-Oates J, et al. The lipid lysyl-phosphatidylglycerol is present in membranes of *Rhizobium tropici* CIAT899 and confers increased resistance to polymyxin B under acidic growth conditions. MPMI. 2007;20:1421–30.
141. Thedieck K, Hain T, Mohamed W, Tindall BJ, Nimtz M, Chakraborty T, et al. The MprF protein is required for lysinylation of phospholipids in listerial membranes and confers resistance to cationic antimicrobial peptides (CAMPs) on Listeria monocytogenes. Mol Microbiol. 2006;62:1325–39.
142. Capo A, Natalello A, Marienhagen J, Pennacchio A, Camarca A, Di Giovanni S, et al. Structural features of the glutamate-binding protein from Corynebacterium glutamicum. Int J Biol Macromol. 2020;162:903–12.
143. Hartl DL, Clark AG. Principles of population genetics, Fourth Edition; 1998.
144. Bing X, Gerlach J, Loeb G, Buchon N. Nutrient-dependent impact of microbes on Drosophila suzukii development. mBio. 2018;9:e02199–17.
145. Keebaugh ES, Yamada R, Obadia B, Ludington WB, Ja WW. Microbial quantity impacts Drosophila nutrition, development, and lifespan. iScience. 2018;4:247–59.
146. Martino ME, Bayjanov JR, Joncour P, Hughes S, Gillet B, Kleerebezem M, et al. Nearly complete genome sequence of Lactobacillus plantarum strain NIZO2877. Genome Announc. 2015;3:e01370–15.
147. Poulsen LK, Licht TR, Rang C, Krogfelt KA, Molin S. Physiological state of Escherichia coli BJ4 growing in the large intestines of streptomycin-treated mice. J Bacteriol. 1995;177:5840–5.
148. Packey CD, Shanahan MT, Manick S, Bower MA, Ellermann M, Tonkonogy SL, et al. Molecular detection of bacterial contamination in gnotobiotic rodent units. Gut Microbes. 2013;4:361–70.

149. Widdel F. Theory and Measurement of Bacterial Growth; 2010.
150. Kushkevych I, Kotrsová V, Dordević D, Buňková L, Vítězová M, Amedei A. Hydrogen sulfide effects on the survival of Lactobacilli with emphasis on the development of inflammatory bowel diseases. Biomolecules. 2019;9:752.
151. Bolger AM, Lohse M, Usadel B. Trimmomatic: a flexible trimmer for Illumina sequence data. Bioinformatics. 2014;30:2114–20.
152. Deatherage DE, Barrick JE. Identification of mutations in laboratory-evolved microbes from next-generation sequencing data using breseq. In: Sun L, Shou W, editors. Engineering and analyzing multicellular systems. New York: Springer New York; 2014. p. 165–88.
153. Huerta-Cepas J, Szklarczyk D, Forslund K, Cook H, Heller D, Walter MC, et al. eggNOG 4.5: a hierarchical orthology framework with improved functional annotations for eukaryotic, prokaryotic and viral sequences. Nucleic Acids Res. 2016;44:D286–93.
154. Lactiplantibacillus plantarum evolution animal hosts, *NCBI*, PRJNA808881. (2022).

Publisher's Note

Springer Nature remains neutral with regard to jurisdictional claims in published maps and institutional affiliations.

Ready to submit your research? Choose BMC and benefit from:

- fast, convenient online submission
- thorough peer review by experienced researchers in your field
- rapid publication on acceptance
- support for research data, including large and complex data types
- gold Open Access which fosters wider collaboration and increased citations
- maximum visibility for your research: over 100M website views per year

At BMC, research is always in progress.

Learn more biomedcentral.com/submissions